BOREAS An international journal of Quaternary research

Re-investigation of the Bispingen palaeolake sediment succession (northern Germany) reveals that the Last Interglacial (Eemian) in northern-central Europe lasted at least ~15 000 years

STEFAN LAUTERBACH, FRANK H. NEUMANN, RIK TJALLINGII AND ACHIM BRAUER

BOREAS

Lauterbach, S., Neumann, F. H., Tjallingii, R. & Brauer, A. 2024 (April): Re-investigation of the Bispingen palaeolake sediment succession (northern Germany) reveals that the Last Interglacial (Eemian) in northern-central Europe lasted at least ~15 000 years. *Boreas*, Vol. 53, pp. 243–261. https://doi.org/10.1111/bor.12649. ISSN 0300-9483.

Investigating past interglacial climatic and environmental changes can enhance our understanding of the natural rates and ranges of climate variability under interglacial boundary conditions. However, comparing past interglacial palaeoclimate records from different regions and archives is often complicated by differing and uncertain chronologies. For instance, the duration of the Last Interglacial in Europe is still controversial as southern European palaeoclimate records suggest a duration of ~16 500–18 000 years, while a length of only ~11 000 years in northern-central Europe was previously inferred from the analysis of partly annually laminated (varved) palaeolake sediments recovered at Bispingen, northern Germany. To resolve this discrepancy, we here present sediment microfacies, geochemistry and pollen data from a new sediment core from the Bispingen palaeolake sediment succession, covering the entire Last Interglacial (Eemian) and the earliest part of the Last Glacial (Weichselian). In particular, we provide evidence that the duration of the Last Interglacial at Bispingen must have been hitherto underestimated due to the investigation of an incomplete sediment core. Using microscopic varve counting and sedimentation rate estimates for non-varved sections on the new sediment core, we show that the Eemian in northern-central Europe probably lasted at least ~15 000 years, about 4000 years longer than previously thought. This new duration estimate is in much better agreement with results from southern European palaeoclimate records, clarifying the enigma of a steep trans-European vegetation gradient for several millennia at the end of the Last Interglacial.

Stefan Lauterbach (slauterbach@leibniz.uni-kiel.de), Institute of Geography and Spatial Organization, Polish Academy of Sciences, 00-818 Warsaw, Poland and Section 4.3 – Climate Dynamics and Landscape Evolution, GFZ German Research Centre for Geosciences, 14473 Potsdam, Germany and Leibniz Laboratory for Radiometric Dating and Stable Isotope Research, Kiel University, 24118 Kiel, Germany; Frank H. Neumann, Unit for Environmental Sciences and Management, Faculty of Natural and Agricultural Science, North-West University, 2531 Potchefstroom, South Africa and Evolutionary Studies Institute, University of the Witwatersrand, 2000 Braamfontein, South Africa and Section Paleontology, Institute for Geosciences, University of Bonn, 53115 Bonn, Germany; Rik Tjallingii, Section 4.3 – Climate Dynamics and Landscape Evolution, GFZ German Research Centre for Geosciences, 14473 Potsdam, Germany; Achim Brauer, Section 4.3 – Climate Dynamics and Landscape Evolution, GFZ German Research Centre for Geosciences, 14473 Potsdam, Germany and Institute of Geosciences, University of Potsdam, 14476 Potsdam, Germany; *received 1st August 2023, accepted 15th January 2024.*

The Last Interglacial, ~125 000 years ago, was characterized by a smaller global ice volume as well as higher air temperatures and sea levels than today (Bintanja *et al.* 2005; Dutton & Lambeck 2012; Fischer *et al.* 2018; Fox-Kemper *et al.* 2021), a function of strong eccentricity-precession forcing despite lower atmospheric CO_2 levels (Schneider *et al.* 2013). As one of the warmest interglacials during the last ~800 000 years (Past Interglacials Working Group of PAGES 2016) and the most recent period with climate conditions similar to those expected in the near future under rising atmospheric greenhouse gas concentrations and continuing global warming, it is therefore suitable to investigate environmental responses to warmer-than-present climate conditions as well as natural rates and ranges of interglacial climate variability. Consequently, numerous palaeoclimate proxy records from this time interval have been obtained from different types of sedimentary archives in Europe and the adjacent North Atlantic. However, the establishment of robust internal chronologies for records from this region as well as their absolute dating and their alignment still pose a major challenge. To date, only very few complete and accurately dated proxy records of Last Interglacial climate variability in Europe are available from speleothems (e.g. Drysdale *et al.* 2005, 2007; Tzedakis *et al.* 2018; Wilcox *et al.* 2020; Luetscher *et al.* 2021) and annually laminated (varved) (palaeo)lake sediments (e.g. Sirocko *et al.* 2005; Brauer *et al.* 2007; Allen & Huntley 2009). In contrast, the vast majority of regional terrestrial palaeoclimate proxy records, mostly originating from non-varved (palaeo)lake sediments, suffers from substantial chronological uncertainties. This includes records that have (i) no age control at all (e.g. Mamakowa 1989; Litt 1994; Kołaczek *et al.* 2012; Bober *et al.* 2018; Malkiewicz 2018a, b; Kupryjanowicz *et al.* 2021; Pidek *et al.* 2021), (ii) only weakly constrained age models (e.g. Hahne *et al.* 1994; Tzedakis *et al.* 2003; Sinopoli *et al.* 2018), or (iii) chronologies that are only based on tentative correlations to marine sediment records (e.g. Kukla *et al.* 1997, 2002a; Milner *et al.* 2013; Salonen *et al.* 2018; Kern *et al.* 2022). In contrast, the chronologies of marine palaeoclimate records from the eastern

DOI 10.1111/bor.12649

North Atlantic rely either on orbital tuning (e.g. Sánchez Goñi *et al.* 1999), the calibration of benthic foraminifera stable oxygen isotope ($\delta^{18}O$) data against radiometrically dated coral and speleothem records of past sea level changes (e.g. Shackleton *et al.* 2002, 2003; Sánchez Goñi *et al.* 2008), or correlation to absolutely dated terrestrial palaeoclimate records (Tzedakis *et al.* 2018). The equivocal reliability, precision and accuracy of these various chronological approaches seriously hamper the reliable alignment of individual proxy records and the robust assessment of the duration of the Last Interglacial at different sites and consequently (i) the reliable quantification of the rates of Last Interglacial climatic and environmental changes and (ii) the identification of regional leads and lags in climate development.

The first estimate for the duration of the Last Interglacial (i.e. the Eemian in northern-central European pollen stratigraphies) in the circum-Atlantic region was based on a tentative correlation between a phase of low foraminifera $\delta^{18}O$ values in North Atlantic sediment cores and the occurrence of interglacial vegetation in Europe. This led to the conclusion that the Last Interglacial comprised only the oldest part of Marine Isotope Stage (MIS) 5, i.e. substage MIS 5e, and had a duration of ~11 000 years (Shackleton 1969). The exact duration and timing of the Last Interglacial in continental Europe remained, however, elusive because the $\delta^{18}O$ analyses on the deep-sea sediments were not accompanied by pollen data. Nevertheless, the idea of a Last Interglacial duration of ~11 000 years was supported shortly thereafter by evidence from the partly varved Eemian palaeolake sediment succession of Bispingen, northern Germany (Müller 1974). In contrast, later studies on pollen records from eastern and southern-central France suggested a substantially longer duration of the Last Interglacial (~19 000–23 000 years) and its extension into MIS 5d (Kukla *et al.* 1997, 2002a, b) as well as a millennia-long vegetation gradient between southern and northern-central Europe at its demise (Kukla *et al.* 2002b; Tzedakis 2003). However, these duration estimates were controversially discussed as they were only based on tentative correlations to the marine $\delta^{18}O$ stratigraphy and not on independent dating (Turner 2002). Since then, considerable progress has been made in refining the chronology of the Last Interglacial in Europe. For instance, parallel pollen and $\delta^{18}O$ analyses on marine sediments from the Iberian margin yielded a length of ~16 400 years for the pollen-defined Last Interglacial and revealed a considerable asynchrony between global ice volume-driven $\delta^{18}O$ changes in the marine realm and terrestrial vegetation development (Sánchez Goñi *et al.* 1999; Shackleton *et al.* 2002, 2003), while pollen data from the varved lake sediment record of Lago Grande di Monticchio, southern Italy, provided evidence for a Last Interglacial duration of 17 700±200 years (Brauer *et al.* 2007; Allen & Huntley 2009). Furthermore, a precisely dated speleothem $\delta^{18}O$ record from Corchia Cave, northern Italy, indicated that the Last Interglacial lasted ~16 600 years (Drysdale *et al.* 2005, 2007), which has recently been revised to ~18 000 years, providing also a new chronological framework for pollen records from the Iberian margin (Tzedakis *et al.* 2018). These latest findings leave the ~50-year-old results from the partly varved Bispingen palaeolake sediment succession, which determine the duration of the Last Interglacial in northern-central Europe to be ~5500–7000 years shorter than further south, as a notable exception. However, whether this reflects chronological deficiencies of the individual records, difficulties in correlating regionally different vegetation successions and/or proxies (e.g. pollen vs. $\delta^{18}O$) or a prolonged vegetation gradient between southern and northern-central Europe at the end of the Last Interglacial, remains unresolved.

To re-evaluate the biostratigraphy and chronology of the Eemian in northern-central Europe we analysed a new sediment core from the Bispingen palaeolake sediment succession. Here we present the results of detailed sediment microfacies analysis, including microscopic varve counting, as well as geochemical and palynological analyses on this sediment core. By comparing these data with results from the classic sediment core KS 186/70 (Müller 1974), we revise the duration estimates of individual pollen zones, establish a new floating chronology for the Eemian in northern Germany and discuss this in relation to other Last Interglacial palaeoclimate records from Europe.

Study area

The Bispingen palaeolake sediment succession is located in northern Germany, ~1.3 km southwest of the village of Bispingen (approx. latitude 53°05′N, longitude 10°00′E) and ~50 km south of Hamburg (Fig. 1). It was discovered in the early 1970s during a large-scale prospection for diatomite deposits and belongs to a series of spatially confined palaeolake sediment successions in the upper valley of the Luhe River, some of which had been exploited for diatomite since the 19th century (Benda & Brandes 1974). The diatomite deposit that is associated with the Bispingen palaeolake sediment succession covers an area of ~0.1 km^2 (estimated volume ~150 000 m^3) and is characterized by a wedge-shaped geometry, reaching maximum thickness in the southeast and rapidly thinning towards the west and north/-northeast, as deduced from a suite of spatially distributed sediment cores obtained during the early 1970s prospection (Benda & Brandes 1974). Detailed pollen analyses on one of these sediment cores (KS 186/70) from the southeastern margin of the palaeolake sediment succession (Fig. 1) revealed that the former lake existed throughout the entire Last Interglacial (Eemian) as well as during the early Last Glacial (Weichselian) (Müller 1974). The similarity of the pollen record to

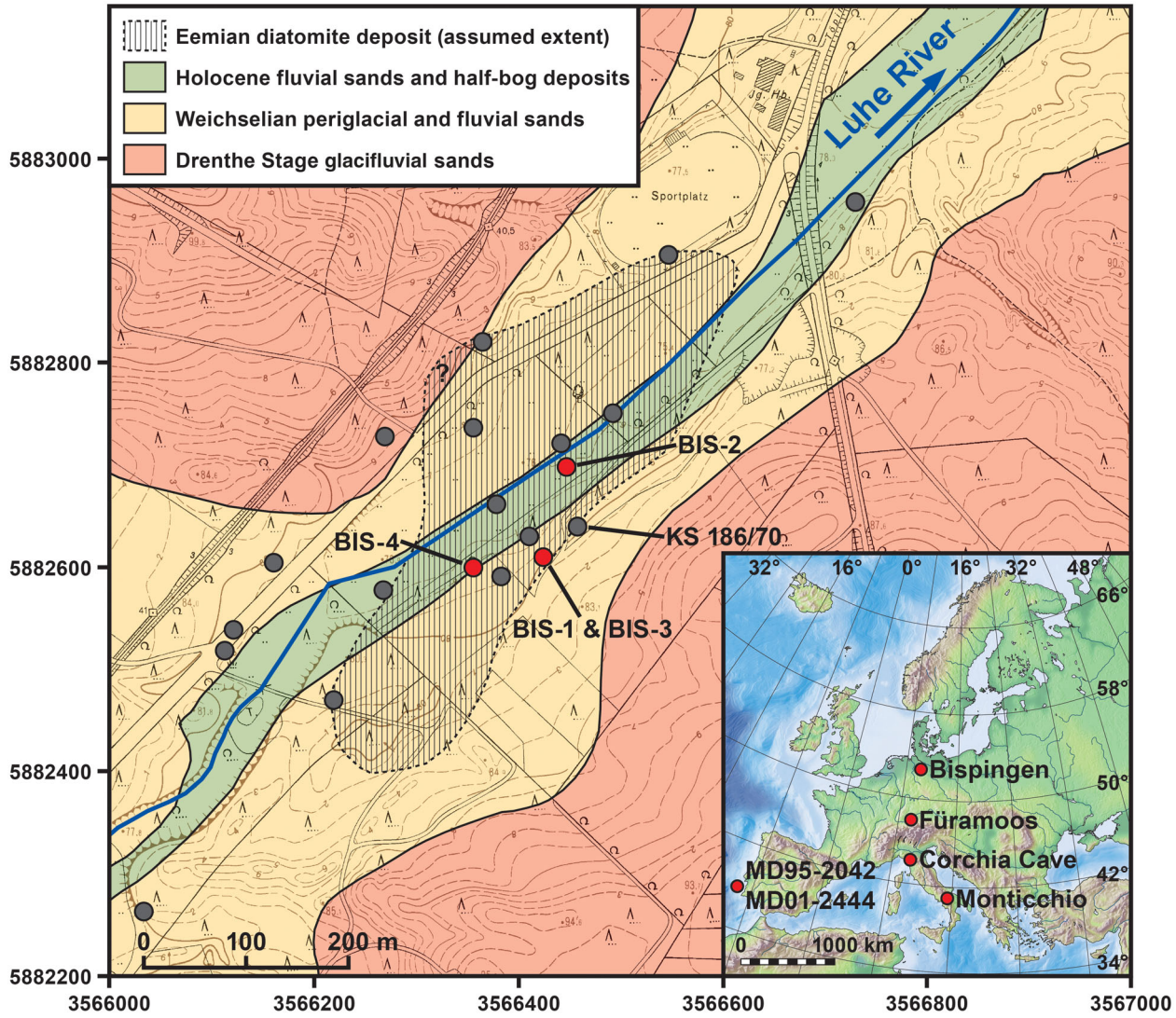

Fig. 1. Topographic and simplified geological map of the surroundings of the Bispingen palaeolake sediment succession in northern Germany (basic topographic map DGK 5, Sheet 2925/12 – Bispingen (zone 3 cartesian Gauss-Krüger coordinates); Lower Saxony State Office for Geographic Information and Land Development, Hanover, Germany). The insert map shows the locations of Bispingen and other Last Interglacial proxy records discussed in the text and displayed in Fig. 8. Positions of the sediment cores obtained in 2000 and the early 1970s (see Benda & Brandes 1974) are indicated by red and grey dots, respectively. The extent of the diatomite deposit as well as geological data and sediment core locations were obtained from the Lower Saxony Soil Information System (NIBIS) map server (Lower Saxony State Office for Mining, Energy and Geology, Hanover, Germany).

other sites in northern-central Europe (e.g. Menke & Tynni 1984; Mamakowa 1989; Hahne *et al.* 1994; Litt 1994; Kołaczek *et al.* 2012; Malkiewicz 2018a, b; Kupryjanowicz *et al.* 2021; Pidek *et al.* 2021; Suchora *et al.* 2022) with respect to characteristic vegetation elements and their succession thereby unequivocally proves the Last Interglacial to early Last Glacial age. The Bispingen palaeolake developed – like all former lakes in the upper valley of the Luhe River – in an ENE–WSW-oriented subglacial meltwater channel that had been formed during the Drenthe Stage ice advance, the main phase of the Penultimate Glacial (Saalian), as indicated by petrographic analysis of the sediments that constitute the hills surrounding the Luhe River valley (Benda & Brandes 1974). As the following Warthe Stage ice advance, the last major glacier advance of the Saalian, did not reach south of Bispingen (Ehlers *et al.* 2004), the then-exposed high-relief subglacial channel was partly filled with reworked glacifluvial sands and gravels during the terminal phase of the Saalian. This initial phase of channel filling was followed by the formation of several small lakes in the remaining basins and the deposition of calcareous muds, gyttjas and diatomites during the Eemian (Benda & Brandes 1974). As the glacier advances of the following Weichselian did not reach the Saalian ice margins (Ehlers *et al.* 2004), all former lake

basins in the upper valley of the Luhe River were covered during the Weichselian by several metres of glacifluvial sands, which are mainly composed of reworked Drenthe Stage material (Benda & Brandes 1974).

Material and methods

Sediment coring and compilation of the BIS-2000 composite sediment core

Four parallel sediment cores, each consisting of several consecutive segments of 1 m length and 100 mm diameter, were recovered by wireline core drilling from four sites across the Bispingen palaeolake sediment succession (Fig. 1) in December 2000. Sites BIS-1 and BIS-3 are located ~1.5 m apart at the eastern margin of the former lake (53°04′17.5″N, 9°59′23.5″E), ~50 m southwest of the classic site KS 186/70 (53°04′18.9″N, 9°59′25.9″E; Benda & Brandes 1974; Müller 1974), whereas sites BIS-2 (53°04′20.8″N, 9°59′24.8″E) and BIS-4 (53°04′17.8″N, 9°59′20.2″E) are located ~65 m north and ~100 m southwest of site KS 186/70, respectively (Fig. 1). Following core retrieval, all core segments were longitudinally split, sedimentologically described and photographed at the GFZ German Research Centre for Geosciences (GFZ) in Potsdam, Germany. Subsequently, a continuous composite sediment core named BIS-2000 (Fig. 2) was compiled by correlating the core segments obtained at sites BIS-1 and BIS-3, which are located closest to the thoroughly studied classic site KS 186/70, via macroscopic marker layers. Where a reliable parallelization of the individual

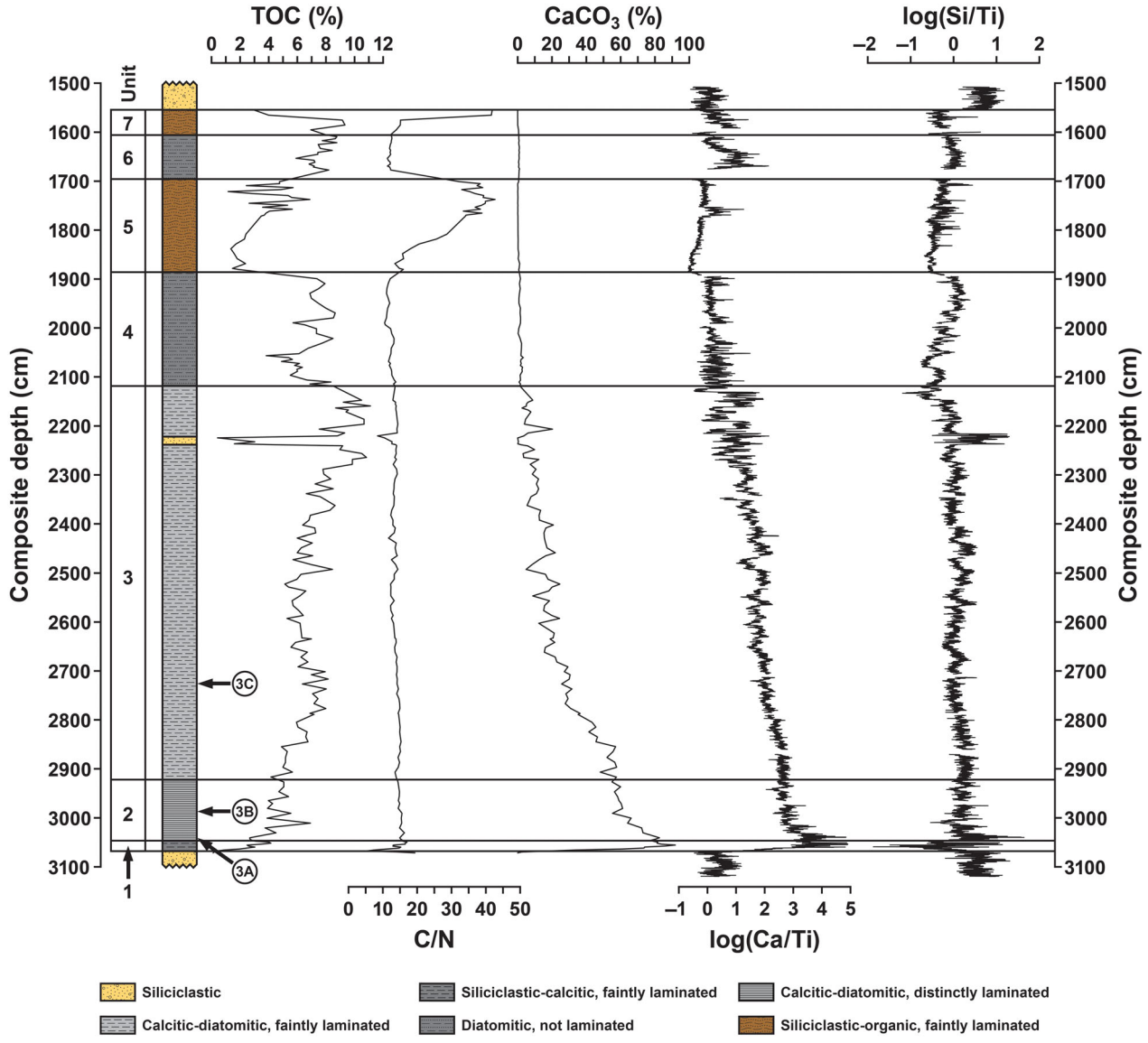

Fig. 2. Sedimentology of the composite sediment core BIS-2000 and results of geochemical analyses. Numbers (3A–3C) next to the stratigraphical column indicate the positions of different varve types displayed in Fig. 3.

core segments from these two sites was impossible, consecutive core segments from site BIS-3 were used for BIS-2000, considering gaps of 2 cm between the consecutive core segments to account for possible sediment loss during core retrieval. BIS-2000 has a total length of 3123 cm and the palaeolake sediments between the basal Saalian and overlying Weichselian sands cover the section between 3068 and 1555 cm (Fig. 2).

Bulk sediment geochemical analyses

Bulk sediment geochemical analyses were carried out at the GFZ on freeze-dried and homogenized sediment samples that were taken from BIS-2000 between 3072 and 1555 cm (n = 200; average sampling resolution 10 cm, locally increased to 2–4 cm). The total inorganic carbon (TIC) content was measured on ~50-mg aliquots by coulometric titration using a STRÖHLEIN Coulomat 702 (CO_2 released by treatment with hot H_2PO_4). As microscopic inspection revealed that calcite is the dominant carbonate mineral in the sediments (see below), the $CaCO_3$ content was calculated stoichiometrically from the TIC content ($CaCO_3$ = TIC × 8.333). Total carbon (TC) and total nitrogen (TN) contents were measured by burning ~100–200 mg aliquots in a LECO CNS-2000 elemental analyser in an oxygen gas flow at 1350 °C and measuring TC and TN contents by infrared and heat conductivity detection, respectively. Total organic carbon (TOC) contents of each sample were finally calculated as the difference between TC and TIC contents. TOC and $CaCO_3$ contents are expressed as per cent of sediment dry weight and the C/N ratio was calculated as the TOC/TN mass ratio.

X-ray fluorescence core scanning

To characterize the element composition of the BIS-2000 sediments, non-destructive X-ray fluorescence (XRF) core scanning was carried out at the GFZ. First, a fresh core surface was prepared for all split core segments of the composite profile, which was covered with foil before XRF measurements were conducted with an ITRAX XRF core scanner. Measurements were performed every 2 mm by irradiating the split core surface with a Rh X-ray source (30 kV, 55 mA) for 15 s. As element intensity records obtained by XRF core scanning provide information about relative changes in element composition that are affected by down-core variations of the physical properties of the sediments, core surface geometry and matrix effects (Tjallingii *et al.* 2007; Weltje & Tjallingii 2008), the geochemical characterization is best presented by log-ratios of the element intensities (Weltje & Tjallingii 2008). Therefore, log-ratios of the silicon, calcium and titanium intensities, i.e. log(Si/Ti) and log(Ca/Ti), are presented here to visualize relative variations in the content of biogenic silica (i.e. diatoms) and calcite with respect to detrital components throughout the sediment record.

Palynological analyses

Pollen analyses on ~1-cm^3 sediment samples from BIS-2000 (n = 138; average sampling resolution 10 cm, locally increased to 2–4 cm), covering the section between 3068 and 1819 cm, were carried out at the University of Bonn, Germany, and subsequently at the University of the Witwatersrand, South Africa. Sample preparation followed the standard method described by Berglund & Ralska-Jasiewiczowa (1986), including treatment with cool HF and HCl, 3 min acetolysis, staining with safranine, and mounting in glycerol. At the University of the Witwatersrand, semi-permanent slides were prepared using glycerine jelly. In total, 442–1016 (median: 517) terrestrial pollen grains per sample were counted using a light microscope at 4000× magnification (100× oil immersion objective). Identification of individual pollen taxa was aided by modern pollen reference collections of central European plants and descriptions of the European pollen flora (Punt 1976; Punt & Clarke 1980, 1981, 1984; Punt *et al.* 1988, 1995, 2003; Punt & Blackmore 1991; Beug 2004). Pollen percentages were calculated following the standard method based on the sum of trees/shrubs (arboreal pollen – AP) and herbs (non-arboreal pollen – NAP; except aquatic and wetland plants) and the pollen diagram was plotted using TILIA (Grimm 1992). Additionally, we applied the percentage calculation originally used for KS 186/70 (*Corylus* and non-tree pollen percentages based on tree pollen values only; Müller 1974). Based on this calculation, the BIS-2000 pollen record was subdivided into individual pollen assemblage and abundance zones (PAAZ; Table 1) following the classic Eemian zonation scheme for northern Germany (Selle 1962). Being exactly the same zonation as used for KS 186/70 (Müller 1974), this enables a direct comparison between the two sediment cores with respect to the thickness/duration of individual PAAZ. However, if not stated otherwise, all pollen percentages presented here are based on the standard method.

Sediment microfacies analysis, varve counting and sedimentation rate estimates

Large-scale petrographic thin sections for sediment microfacies analysis were prepared at the GFZ according to the method described by Brauer *et al.* (1999) from sediment slabs (100 × 20 × 10 mm) that were taken continuously from the core segments included in BIS-2000. Microscopic analyses were carried out at different magnifications (25–400×) and optical conditions (plane- and cross-polarized light, dark field illumination) using a NIKON SMZ-U stereoscopic microscope and a ZEISS Axiophot polarization microscope.

To establish a floating chronology for BIS-2000, microscopic varve counting was carried out between 3047 and 2922 cm. Within this section, varves were counted three times and classified into three categories according to their preservation state and the variance between the individual counts: (i) sections with well-preserved and clearly distinguishable varves (no variance between individual counts and therefore negligible counting uncertainty), (ii) varved sections where the discrimination of the boundaries of individual varves was partly difficult (5% counting uncertainty), and (iii) faintly varved sections, where the discrimination of individual varve boundaries was hardly possible and the number of varves was interpolated using the average varve thickness/sedimentation rate of adjacent well-varved sections (estimated uncertainty 20%). The results of microscopic varve counting (including local varve thickness-based interpolation) were used to determine the duration of individual PAAZ in the section 3057–2891 cm (see sections 'Sediment microfacies, varve counting and sedimentation rate estimates' and 'Pollen zonation and duration of individual PAAZ'). In contrast, to determine the duration of individual PAAZ below 3057 cm and between 2891 and 2046 cm, i.e. in sections of BIS-2000 where reliable varve counting was not possible, we used for convenience exactly the same average sedimentation rates as deduced for these PAAZ from their thickness and estimated duration in KS 186/70 (Müller 1974) (see Table 2 and sections 'Sediment microfacies, varve counting and sedimentation rate estimates' and 'Pollen zonation and duration of individual PAAZ').

Results and interpretation

Sediment composition and geochemistry

Based on sediment composition, geochemistry and microfacies, seven sedimentological units (1 to 7 from bottom to top) can be distinguished in BIS-2000 between 3068 and 1555 cm (Fig. 2).

Unit 1 (3068–3047 cm) is composed of dark brownish grey calcite mud. It represents the initial stage of lacustrine sedimentation and directly overlies yellowish grey, fine to medium sands with occasionally intercalated coarse sand and gravel layers that were deposited during the Saalian (see Benda & Brandes 1974). The main characteristic of unit 1 is the distinct increase in $CaCO_3$ from ~2% at the base to ~80–90% at the top, also reflected by rapidly increasing log(Ca/Ti) values (Fig. 2). However, the sediments still contain abundant reworked fine sand- to clay-sized siliciclastics (mainly quartz and feldspar). Further components are diatoms and amorphous organic matter (TOC ~1–4%; Fig. 2) as well as µm-scale pyrite framboids, which occur finely dispersed within the matrix above 3055 cm.

Unit 2 (3047–2922 cm) consists of brownish grey calcite mud that is, in contrast to unit 1, characterized by a distinct and mostly well-preserved sub-mm-scale light–dark lamination (Fig. 3A, B). $CaCO_3$ gradually decreases from >80 to ~60%, also reflected by a decrease in log(Ca/Ti), while the TOC content ranges between ~3 and ~5% (Fig. 2). C/N values of ~15 (Fig. 2) indicate that the organic matter consists of a mixture of algae, aquatic macrophytes and higher terrestrial plants (see Meyers & Lallier-Vergès 1999). Diatoms become increasingly abundant while the amount of silt- to clay-sized siliciclastics distinctly decreases. Nest-like aggregates of µm-scale pyrite framboids, partly forming discrete layers of ~50–100 µm thickness, are frequent in the lower part of unit 2.

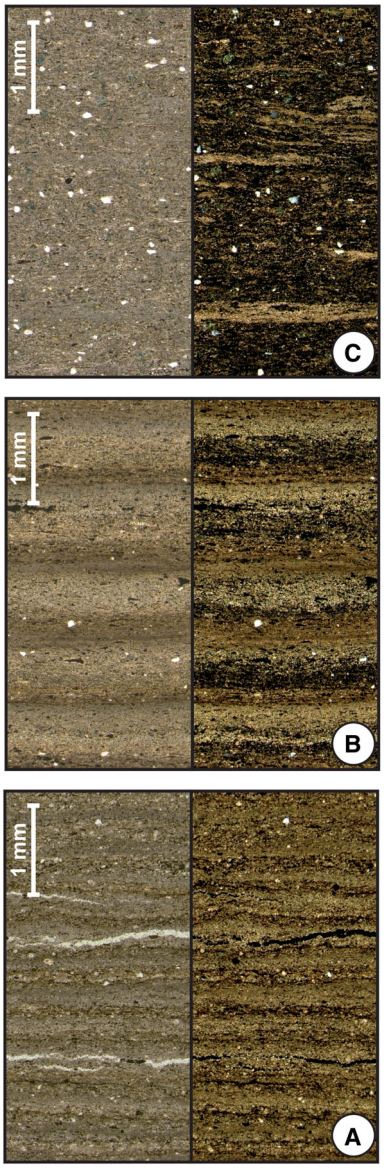

Fig. 3. Thin section images of different varve types in BIS-2000 (left side: plane-polarized light, right side: cross-polarized light). A. Unit 2/PAAZ IIa (~3041 cm). B. Unit 2/PAAZ IIIa (~2987 cm). C. Unit 3/PAAZ IVa (~2726 cm).

The boundary to unit 3 (2922–2129 cm), which is composed of calcitic diatomite, is defined by the disappearance of the continuous sub-mm-scale light–dark lamination; instead, occasional diatom layers and calcite lenses form a faint lamination (Fig. 3C). $CaCO_3$ remains at ~50–60% until ~2850 cm, followed by a distinct decrease to ~30% between ~2850 and ~2770 cm and a subsequent gradual decrease to ~3% at the top of unit 3, also reflected by gradually decreasing log(Ca/Ti) values (Fig. 2). The decreasing calcite content is accompanied by a gradual change in sediment colour from brownish grey to dark greyish brown. In contrast, the diatom content remains relatively constant throughout unit 3, reflected by stable log(Si/Ti) values (Fig. 2), and also the content of amorphous organic material and plant debris (TOC ~5–11%) as well as the C/N values (~12–15) remain largely unchanged (Fig. 2). Only very few silt- to clay-sized siliciclastics as well as pyrite are diffusely dispersed within the sediment and above 2879 cm vivianite occurs. An intercalated sand layer at 2239–2221 cm with lumps of regular lacustrine sediment most likely reflects instantaneous input of catchment material that apparently dislocated lacustrine sediments from the basin slope. Relatively high log(Si/Ti) values across the sand layer (Fig. 2) are related to its high quartz content, obscuring the reflection of the otherwise largely constant diatom content by log(Si/Ti).

Unit 4 (2129–1886 cm) is composed of non-laminated, dark brown diatomite that is still relatively organic-rich (TOC ~5–9%) but, in contrast to unit 3, virtually calcite-free ($CaCO_3$ ~1–3%), which is also reflected by lower log(Ca/Ti) values (Fig. 2). Diatoms are still abundant as indicated by largely unchanged log(Si/Ti) values (Fig. 2) and horizontally bedded organic macro-remains as well as very few finely dispersed siliciclastics, pyrite and vivianite occur, the latter occasionally forming discrete layers of up to 1 mm thickness.

Subunit 5a (1886–1849 cm) is characterized by a faint mm-scale alternation of clayey-siliciclastic and organic-detrital layers, indicating a significantly changed depositional environment. The organic matter content is lower (TOC <6%) than in unit 4 (Fig. 2), vivianite is absent, but diatoms are still abundant. The disappearance of diatoms in overlying subunit 5b (1849–1697 cm) apparently marks the end of lacustrine deposition. Sediments in this subunit are characterized by a cm-scale alternation of layers that contain silt-sized siliciclastics mixed with fine-grained organic material and layers that consist of sand mixed with coarse plant debris. The increasing contribution of terrestrial plant material is reflected by a gradual C/N increase from ~15 to >30 (Fig. 2; see Meyers & Lallier-Vergès 1999), while slightly higher log(Si/Ti) values reflect the increased amount of siliciclastics in absence of diatoms. Strong variations in TOC (~1–6%) above 1771 cm reflect the random sampling of either more clastic or more organic layers.

Unit 6 (1697–1606 cm) is characterized by another sharp shift in sediment composition. Following the deposition of mixed organic-clastic sediments in subunit 5b, the recurrence of diatoms and vivianite in unit 6 most likely reflects the recommencement of lacustrine sedimentation. The amount of fine-grained siliciclastics and coarse-grained organic debris, both scattered within the dark brown to greyish brown diatomite, is lower than in subunits 5a and 5b. TOC values of ~6–9% (Fig. 2) mainly reflect amorphous organic matter.

The boundary to unit 7 (1606–1555 cm) is characterized by an abrupt re-increase in the amount of siliciclastics and organic macro-remains, deposited as alternating mm-scale layers of either silt-sized siliciclastics or organic debris. Diatoms occur only sporadically, partly as discrete mm-scale layers, up to 1569 cm. The subsequent disappearance of diatoms together with a drop in TOC from >9 to <4% (Fig. 2) and an increase in siliciclastics most likely reflects the terminal silting-up of the lake. This is corroborated by relatively high C/N values (>40) in the upper part of unit 7 (Fig. 2), indicating a strong contribution of higher terrestrial plants (see Meyers & Lallier-Vergès 1999).

Above 1555 cm, the lacustrine sediments are covered by yellowish to light grey, quartz-rich fine to medium sands (reflected by high log(Si/Ti) values) with some intercalated organic-rich layers, which were deposited during the Weichselian (see Benda & Brandes 1974).

Sediment microfacies, varve counting and sedimentation rate estimates

The sediments of unit 2 in the basal part of BIS-2000 are characterized by a distinct sub-mm-scale light–dark lamination. The first well-defined light–dark laminae couplets occur between 3047 and 3024 cm and each couplet in this section is composed of two sublayers (Fig. 3A). The basal light sublayer contains, besides some diatoms, mostly micritic calcite. As biogeochemical calcite precipitation is mainly driven by (i) a shift in the $CaCO_3/H_2CO_3$ balance due to photosynthetic removal of CO_2 from the water by algal blooms in early spring and (ii) rising water temperature, affecting the solubility of CO_2 in the water and hence its $CaCO_3$ saturation (Brunskill 1969; Kelts & Hsü 1978; Zolitschka *et al.* 2015), the calcite sublayer is interpreted to represent late spring and summer deposition. The distinct upward grading of the calcite crystals (e.g. Geyh *et al.* 1971; Kelts & Hsü 1978; Lotter 1989; Brauer *et al.* 2008) most likely reflects gradually changing saturation levels during the period of calcite precipitation (Brauer 2004), the successive deposition of coarse- to fine-grained calcite crystals due to size-dependent sinking velocity, and/or the partial dissolution of the fine-grained crystals during sinking (Kelts & Hsü 1978). The overlying dark sublayer contains in contrast to the light sublayer predominantly organic material and some siliciclastics

as well as abundant pyrite framboids, which are likely early diagenetic and partly form discrete layers (Fig. 3A). This sublayer is interpreted to represent deposition during autumn and early spring. In general, the light sublayers are almost twice as thick as the dark sublayers and the thickness of the laminae couplets ranges between ~0.4 and >1.0 mm with thinner couplets at the base of this section.

Between 3024 and 3002 cm, the abundance of diatoms strongly increases and discrete diatom sublayers are occasionally observed below the calcite sublayers. However, the laminae couplets in this section are relatively poorly preserved and the boundaries between individual sublayers are mostly faint.

Above this poorly laminated section, a different laminae microfacies with three instead of two sublayers is observed between 3002 and 2922 cm (Figs 3B, 4) (Tables 1, 2). The sublayer succession thereby resembles that of laminated lake sediments from northern Germany and Poland, where seasonally different deposition was proven by sediment trap studies (see Roeser *et al.* 2021). The base of each sublayer succession in this section is formed by a light diatom sublayer with only very little biogeochemically precipitated calcite (Figs 3B, 4). It is consequently considered to reflect early spring diatom growth in response to increased nutrient availability following spring circulation (Bluszcz *et al.* 2008; Maier *et al.* 2018) and rising air and water temperatures (Zolitschka *et al.* 2015). The light diatom sublayer is overlain by another light sublayer that is composed of biochemically precipitated micritic calcite. It is similar to the calcite sublayers observed between 3047 and 3024 cm (Figs 3B, 4) and consequently interpreted to also reflect deposition during late spring and summer. The calcite sublayer is again overlain by a dark sublayer that mainly contains amorphous organic matter but only little calcite and few diatoms

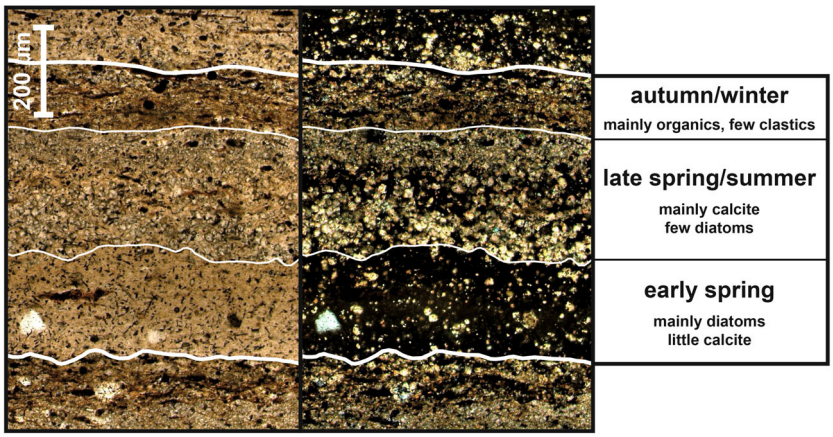

Fig. 4. Thin section image of a typical varve in unit 2/PAAZ IIIa (~2984 cm) with distinct sublayers (left side: plane-polarized light, right side: cross-polarized light).

Table 1. Pollen zonation of the Eemian in northern Germany applied to sediment cores KS 186/70 (Müller 1974) and BIS-2000 (this study) from the Bispingen palaeolake sediment succession.

PAAZ		Definition upper boundary (Müller 1974)	KS 186/70 depth (cm; Müller 1974)	BIS-2000 depth (cm; this study)
VIb	Moderate NAP–*Betula*–*Pinus*	Increase of NAP to >25%	1905–2017	2046–2134
VIa	*Picea*–*Pinus*	Intersection of *Betula* & *Picea* curves; increase of NAP to >5%	2017–2053	2134–2175
Vb	*Pinus*–*Picea*–*Abies*	Decrease of *Abies* to <1%	2053–2103	2175–2269
Va	*Pinus*–*Picea*–*Carpinus*	Increase of *Abies* to >2%	2103–2160	2269–2303
IV	*Carpinus*	Intersection of *Carpinus* & *Picea*/*Pinus* curves	2160–2400	2303–2731
IIIc	*Tilia*–*Ulmus*–*Corylus*	Intersection of *Tilia* & *Carpinus* curves	2400–2463	2731–2891
$IIIb_2$	*Corylus*	Onset increase of *Tilia* to >2%	2463–2498	2891–2975[1]
$IIIb_1$	*Corylus*	Decrease of *Corylus* to <100%	2498–2557	
IIIa	*Quercetum* mixtum–*Corylus*	Increase of *Corylus* to >100%	2557–2593	2975–3005
IIb	*Pinus*–*Quercetum* mixtum	Intersection of *Quercus* & *Corylus* curves	2593–2640	3005–3035
IIa	*Pinus*–*Betula*	Intersection of *Quercetum* mixtum & *Betula* curves	2640–2661	3035–3057
I	*Betula*	Intersection of *Betula* & *Pinus* curves; increase of *Quercetum* mixtum to >1%	2661–2668	3057–3068

[1]A distinction into PAAZ $IIIb_1$ and PAAZ $IIIb_2$ was not made for BIS-2000.

Table 2. Thickness, duration and sedimentation rate for individual PAAZ in KS 186/70 (Müller 1974) and BIS-2000 (this study). The PAAZ nomenclature follows the scheme established by Selle (1962) and used by Müller (1974) for KS 186/70 (see Table 1).

PAAZ	Thickness KS 186/70 (cm)	Duration KS 186/70 (years)	Average sedimentation rate, KS 186/70 (mm a^{-1})	Thickness BIS-2000 (cm)	Duration BIS-2000 (years)	Average sedimentation rate BIS-2000 (mm a^{-1})
VIb	112	2000	0.740	88	1189[3]	0.740[3]
VIa	36			41	554[3]	
Vb	50	2000	0.535	76[2]	1421[3]	0.535[3]
Va	57			34	636[3]	
IV	240	4000	0.600	428	7133[3]	0.600[3]
IIIc	63	705[1]	0.891	160	1796[3]	0.891[3]
$IIIb_2$	35	395[1]	0.891	84	975[4]	0.862[4]
$IIIb_1$	59	700	0.843			
IIIa	36	450	0.800	30	406	0.739
IIb	47	450	1.044	30	352	0.852
IIa	21	200	1.050	22	365[5]	0.603[5]
I	7	100	0.700	11	157[3]	0.700[3]
Total	763	11 000		1022	14 984	

[1]The original duration estimate for PAAZ $IIIb_2$ + IIIc is 1000–1200 years (Müller 1974).
[2]The sand layer between 2239 and 2221 cm was subtracted from the total thickness (94 cm) of PAAZ Vb in BIS-2000.
[3]The average sedimentation rate calculated from the thickness and estimated duration of the PAAZ in KS 186/70 was adopted to calculate the duration of the respective PAAZ in BIS-2000.
[4]Varve counting between 2975 and 2922 cm yielded 615 years. For the remaining upper part of PAAZ IIIb (2891–2922 cm), the number of years was interpolated using the same average sedimentation rate as below 2922 cm (0.862 mm a^{-1}), yielding 360 years.
[5]Varve counting between 3047 and 3035 cm yielded 199 years. For the remaining lower part of PAAZ IIa (3047–3057 cm), the number of years was interpolated using the same average sedimentation rate as above 3047 cm (0.603 mm a^{-1}), yielding 166 years.

(Figs 3B, 4). This sublayer is interpreted to reflect resuspension processes during the autumn and winter stagnation period (see Roeser *et al.* 2021). The average thickness of the laminae couplets in this section is ~0.8 mm and couplets become slightly thicker (~1.0 mm) towards the top, being mainly related to a thickening of the dark sublayers.

Based on the composition and succession of the individual sublayers, which are similar to those of proven annually laminated sediments from other (palaeo)lakes in carbonate-rich catchments (e.g. Geyh *et al.* 1971; Kelts & Hsü 1978; Lotter 1989; Brauer *et al.* 2008; Lauterbach *et al.* 2011, 2019; Tylmann *et al.* 2013; Roeser *et al.* 2021), the sub-mm-scale light–dark laminae couplets in the basal part of BIS-2000 can be classified as carbonaceous-biogenic varves (see Zolitschka *et al.* 2015). Microscopic counting across the entire section between 3047 and 2922 cm revealed 1572±160 varves. This includes 308±45 varves between 3047 and 3024 cm, 275±46 varves in the poorly laminated section between 3024 and 3002 cm and 989±69 varves between 3002 and 2922 cm. These results were in the following applied to the pollen zonation of BIS-2000 to infer the duration of individual PAAZ in the distinctly varved lower part of the sediment succession (see section 'Pollen zonation and duration of individual PAAZ').

In contrast, the duration of individual PAAZ in the faintly/non-varved parts of BIS-2000 (below 3047 cm and between 2891 and 2046 cm) was determined by adopting the average sedimentation rate estimates for these PAAZ from KS 186/70 (Müller 1974; Table 1). Based on local varve counts in PAAZ IIIc and the observation that the ratio between diatoms and organic matter in the faintly/non-varved middle and upper part of KS 186/70 (PAAZ IV–VIb) remained fairly constant while the calcite content concomitantly decreased, Müller (1974) assumed lower sedimentation rates for the PAAZ IV–VIb section than for the varved part of KS 186/70 (PAAZ IIa–IIIc). Geochemical analyses on the BIS-2000 sediments indicate that, in agreement with the observation of Müller (1974), the proportions of organic matter, diatoms and siliciclastics remain also more or less stable in the middle and upper part of the sediment succession, i.e. between ~2850 and 2046 cm (Fig. 2). In contrast, the calcite content continuously decreases from ~55–65% at ~3000–2850 cm (including the uppermost part of the distinctly varved section) to ~30% at ~2770–2700 cm and further to ~10–30% at ~2700–2300 cm, ~5–10% at ~2300–2130 cm and <3% above ~2130 cm (Fig. 2). Due to the consistent sedimentological/geochemical evidence from BIS-2000 and KS 186/70, we therefore also assume lower sedimentation rates for the faintly/non-varved section of BIS-2000 above ~2700 cm and adopted for the PAAZ in this interval for convenience the same average sedimentation rates as those calculated from the thickness and estimated duration of the respective PAAZ in KS 186/70 (Table 2; Müller 1974).

Pollen zonation and duration of individual PAAZ

Using the same zonation criteria as for KS 186/70 (Müller 1974; Table 1), the pollen diagram for the

analysed part of BIS-2000 (3068–1819 cm) can be divided into six local PAAZ (I to VI from bottom to top; including subzones). It reveals a complete Eemian to early Weichselian vegetation succession (Figs 5, S1) that largely resembles the pollen record of KS 186/70 (Müller 1974; Figs 6, S2) and other sites in northern-central Europe (e.g. Menke & Tynni 1984; Mamakowa 1989; Hahne *et al.* 1994; Litt 1994; Kołaczek *et al.* 2012; Malkiewicz 2018a, b; Kupryjanowicz *et al.* 2021; Pidek *et al.* 2021; Kern *et al.* 2022; Suchora *et al.* 2022). As a detailed interpretation of the palynological results in terms of climatic/environmental changes is beyond the scope of the present study, the pollen data are used here only for the biostratigraphical characterization of the Eemian deposits and the establishment of a chronology.

PAAZ I (*Betula*; 3068–3057 cm) is characterized by high percentages of *Betula* (~45–58%) and *Pinus* (~20–49%) as well as decreasing *Juniperus* and *Salix* percentages (Fig. 5), reflecting the spread of pioneer forests at the onset of the Eemian. Open-land indicators, most prominently Poaceae, fluctuate but generally decrease from ~13 to ~7% (Fig. 5). Grassy communities with *Artemisia* dominate in drier habitats, whereas wetter habitats are characterized by Cyperaceae and ferns. The boundary to PAAZ IIa is defined by the intersection of the *Betula* and *Pinus* pollen curves and the increase of *Quercus* and *Ulmus* to >1% (Müller 1974; Table 1). Using the same average sedimentation rate as in KS 186/70 (~0.70 mm a^{-1}; see section 'Sediment microfacies, varve counting and sedimentation rate estimates'), PAAZ I lasted ~160 years (Table 2).

PAAZ IIa (*Pinus–Betula*; 3057–3035 cm) is characterized by high *Pinus* percentages (~70%) and a parallel decrease of *Betula* from ~39 to ~21%, reflecting the replacement of pioneer woodlands by boreal forests (Fig. 5). Gradual soil stabilization due to the spread of boreal forests could explain the decreasing content of allochthonous siliciclastics at the transition between sedimentological units 1 and 2 (3047 cm). *Quercus* spreads and reaches ~3%, whereas *Salix* and *Juniperus* are only weakly present (Fig. 5). As already observed by Müller (1974), *Ulmus* increases before *Quercus* and reaches ~2–9%. *Fraxinus* generally remains <1% and open-land indicators, including grasses, reach a maximum of ~3%. The boundary to PAAZ IIb is defined by the intersection of the *Betula* and mixed oak forest pollen curves (Müller 1974; Table 1). Microscopic varve counting, including varve thickness-based interpolation for the lowermost 10 cm, yielded a duration of 365 years for PAAZ IIa (Table 2).

PAAZ IIb (*Pinus–Quercetum* mixtum; 3035–3005 cm) is characterized by mixed oak forests (*Quercus* ~18–24%) with a still high portion of *Pinus* (~42–55%). *Ulmus* and

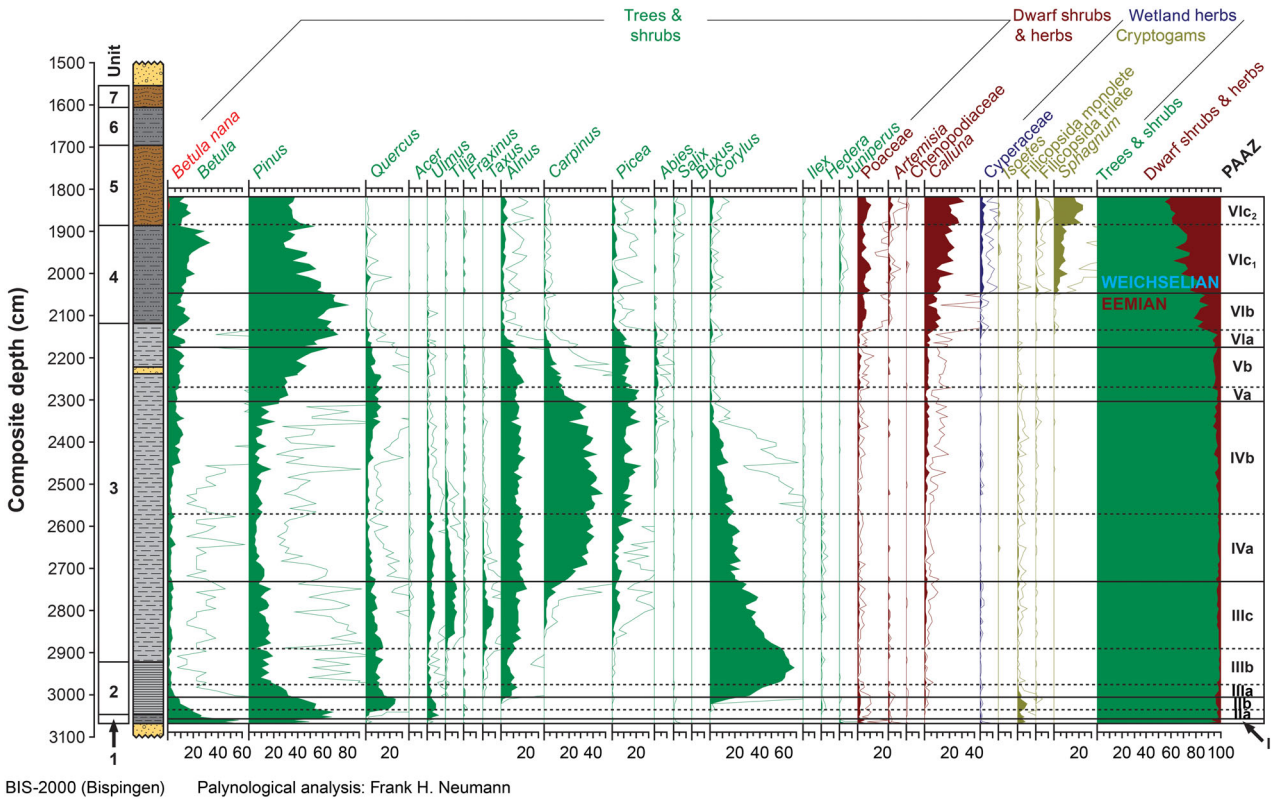

Fig. 5. Simplified pollen diagram of BIS-2000 applying the standard percentage calculation. The boundaries of individual PAAZ follow the criteria used for KS 186/70 (Müller 1974; Table 1). Lithological symbols as in Fig. 2.

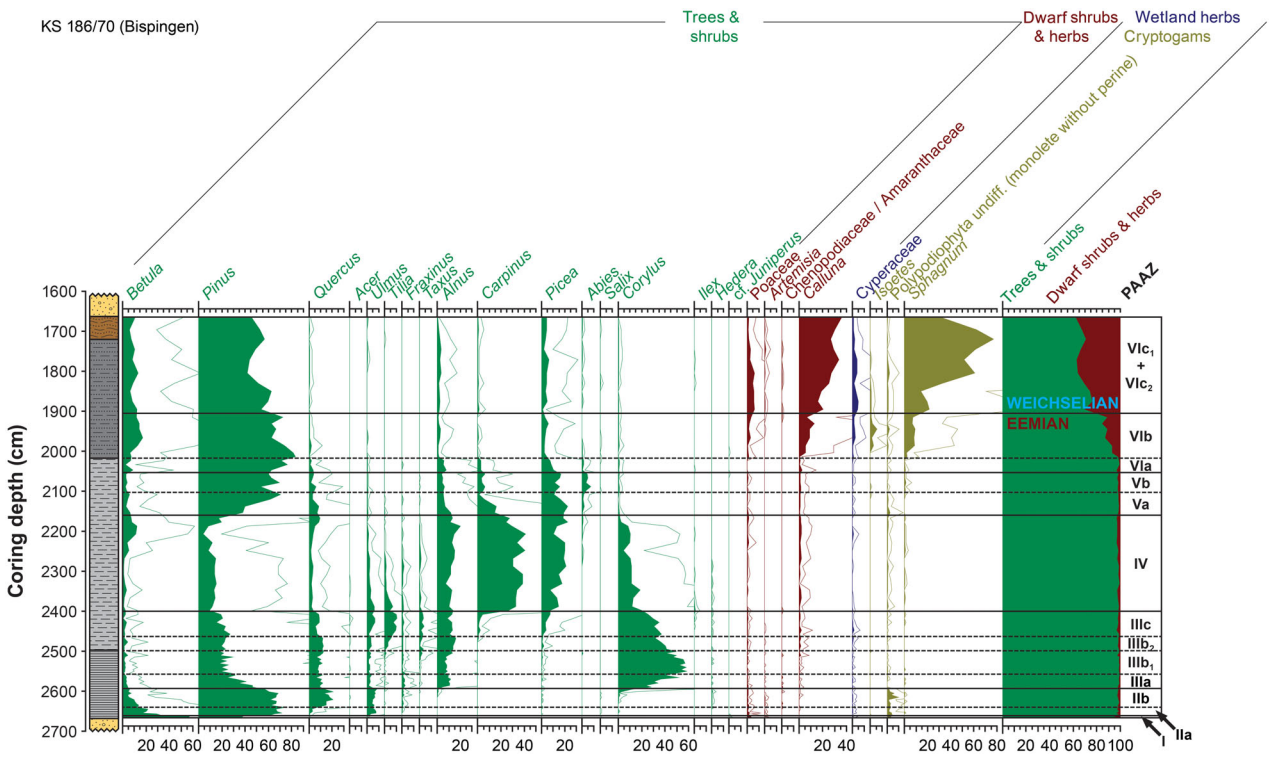

Fig. 6. Simplified pollen diagram of KS 186/70 (Müller 1974) applying the standard percentage calculation. The boundaries of individual PAAZ follow the criteria used for the original pollen diagram of KS 186/70 (Müller 1974; Table 1). The pollen count data are available at the European Pollen Database (https://epdweblog.org) via the Neotoma Paleoecology Database (http://www.neotomadb.org; dataset ID 40169). Lithological symbols as in Fig. 2.

Betula decrease from ~7 to ~4% and from ~18 to ~9%, respectively. *Corylus* increases from <1 to ~15% while herbs remain <4% and *Alnus* reaches ~1% (Fig. 5). The boundary to PAAZ IIIa is defined by the intersection of the mixed oak forest and *Corylus* pollen curves (Müller 1974; Table 1). According to the results of microscopic varve counting, PAAZ IIb lasted 352 years (Table 2).

PAAZ IIIa (*Quercetum* mixtum–*Corylus*; 3005–2975 cm) is characterized by a steep increase of *Corylus* from ~15 to ~42%, while *Pinus* drops to <30% and *Ulmus* and *Quercus* moderately decrease (Fig. 5). *Alnus* culminates at the end of PAAZ IIIa and *Tilia* and *Taxus* are recorded for the first time. Following the percentage calculation applied to KS 186/70 (Müller 1974; Table 1), the boundary to PAAZ IIIb is defined by the increase of *Corylus* to >100% (Figs S1, S2). Applying this calculation method to BIS-2000, similar *Corylus* percentages are reached at the top of PAAZ IIIa (Fig. S1). As inferred from microscopic varve counting, PAAZ IIIa lasted 406 years (Table 2).

PAAZ IIIb (*Corylus*; 2975–2891 cm) is characterized by the continuing replacement of mixed pine forests (*Pinus* ~10–18%) by thermophilous elements (*Quercus*, *Ulmus*, *Corylus*), which already started in PAAZ IIIa (Fig. 5). *Corylus* reaches its highest percentages (~68%) while *Alnus*, *Ulmus* and *Betula* percentages remain similar compared to the top of PAAZ IIIa and *Tilia* and *Taxus* increase to ~1 and ~2%, respectively. The boundary to PAAZ IIIc is defined by the increase of *Tilia* to >2% (Müller 1974; Table 1). Microscopic varve counting, including varve thickness-based interpolation for the uppermost 31 cm, yielded a duration of 965 years for PAAZ IIIb (Table 2).

PAAZ IIIc (*Tilia–Ulmus–Corylus*; 2891–2731 cm) is characterized by the decline of *Corylus* to <30% and a parallel culmination of *Taxus* (maximum ~9%), *Tilia* (maximum ~9%) and *Ulmus* (maximum ~6%) (Fig. 5). *Quercus* gradually decreases while *Pinus* and *Alnus* fluctuate around ~15% and *Betula* percentages are low (~2–4%). *Picea* (maximum ~7%) spreads earlier than *Carpinus*, which markedly increases at the end of PAAZ IIIc (maximum ~12%). *Hedera* is more common and *Ilex*, indicative of oceanic climate conditions and sensitive to low mean January temperatures (Iversen 1944; Zagwijn 1996), is detected for the first time. The boundary to PAAZ IV is defined by the intersection of the *Tilia* and *Carpinus* pollen curves (Müller 1974; Table 1). Using the same average sedimentation rate as in KS 186/70 (~0.89 mm a^{-1}; see section 'Sediment microfacies, varve counting and sedimentation rate estimates'), PAAZ IIIc lasted ~1800 years (Table 2).

PAAZ IV (*Carpinus*; 2731–2303 cm) can be subdivided into a lower (PAAZ IVa; 2731–2571 cm) and an

upper part (PAAZ IVb; 2571–2303 cm), separated by a weakly defined *Carpinus* minimum and a parallel *Picea* increase (Müller 1974). PAAZ IVa represents the late-temperate phase of the Eemian and is characterized by the expansion of *Carpinus* (from ~18 to 35–40%) and *Picea* (from ~6 to ~17%). Parallel, a decline of *Quercus*, *Ulmus*, *Corylus*, *Taxus* and *Tilia* is observed (Fig. 5). *Ilex* and *Hedera* are well distributed, suggesting high summer temperatures and oceanic climate conditions (e.g. Malkiewicz 2018a, b). Low percentages of dwarf shrubs, herbs and wetland elements indicate a closed forest canopy. The overlying PAAZ IVb is characterized by the strongest presence of *Carpinus* (maximum ~48%) and *Picea* (maximum ~24%) and a steady increase of the *Betula* and *Quercus* percentages. *Corylus*, *Ulmus* and *Tilia* percentages decline and oceanic components (*Ilex*, *Hedera*, *Buxus*) occur only sporadically. *Calluna*, regularly present with up to 4%, reflects the presence of a reed belt. The boundary to PAAZ Va is marked by the intersection of the *Carpinus* pollen curve with the *Pinus* and *Picea* pollen curves (Müller 1974; Table 1). Applying the same average sedimentation rate as in KS 186/70 (~0.60 mm a^{-1}; see section 'Sediment microfacies, varve counting and sedimentation rate estimates'), PAAZ IV lasted ~7130 years (Table 2).

PAAZ Va (*Pinus–Picea–Carpinus*; 2303–2269 cm) is characterized by the spread of *Pinus* (from ~24 to ~30%) and the parallel decline of *Carpinus* (from ~22 to ~13%), while *Picea* is still present with up to 21% (Fig. 5). The boundary to PAAZ Vb is defined by the increase of *Abies* to >2% (Müller 1974; Table 1). Using the same average sedimentation rate as in KS 186/70 (~0.54 mm a^{-1}; see section 'Sediment microfacies, varve counting and sedimentation rate estimates'), PAAZ Va is considered to have lasted ~640 years (Table 2).

PAAZ Vb (*Pinus–Picea–Abies*; 2269–2175 cm) reveals a further increase of *Pinus* (from ~30 to ~66%), a strong presence of *Picea* (~8–15%) and a notably high abundance of *Abies* (maximum ~3%) (Fig. 5). *Alnus*, *Carpinus* and *Quercus* percentages gradually decrease and oceanic components are absent except for a few isolated *Hedera* pollen grains. The successive spread of boreal elements likely reflects deteriorating climate conditions (e.g. Malkiewicz 2018a, b). The boundary to PAAZ VIa is defined by the decrease of *Abies* to <1% (Müller 1974; Table 1). With the same average sedimentation rate as in KS 186/70 (~0.54 mm a^{-1}; see section 'Sediment microfacies, varve counting and sedimentation rate estimates'), PAAZ Vb is estimated to have lasted ~1420 years (Table 2).

PAAZ VIa (*Picea–Pinus*; 2175–2134 cm) reflects the terminal phase of the Eemian and is characterized by a major decline of thermophilous elements. *Pinus* increases to ~76%, while *Picea* decreases to ~9%, *Carpinus* and *Quercus* drop to <5% and *Alnus* decreases to <10% (Fig. 5). Dwarf shrubs and herbs fluctuate around 5% while *Calluna* increases to ~4%. The boundary to PAAZ VIb is defined by the intersection of the *Betula* and *Picea* pollen curves and the increase of dwarf shrubs and herbs (NAP) to >5% (Müller 1974; Table 1). Although NAP values already varied between ~3 and ~6% in PAAZ Vb when applying the percentage calculation of Müller (1974) (Fig. S1), we placed the upper boundary of PAAZ VIa only at the significant NAP increase between 2145 and 2124 cm. Using the same average sedimentation rate as in KS 186/70 (~0.74 mm a^{-1}; see section 'Sediment microfacies, varve counting and sedimentation rate estimates'), PAAZ VIa lasted ~550 years (Table 2).

PAAZ VIb (moderate NAP–*Betula–Pinus*; 2134–2046 cm) is dominated by *Pinus*, reaching ~55–80% (Fig. 5). *Betula* percentages gradually increase and dwarf shrubs and herbs also spread. *Picea* decreases to <2% and thermophilous trees (*Carpinus*, *Corylus*, *Alnus*) are only detected at low abundances, whereas *Calluna* (maximum ~13%) and Poaceae (~3–6%) contribute significantly to the pollen spectrum (Fig. 5). The establishment of a boreal *Pinus-Betula-Calluna* heathland reflects a continuing temperature decline (Kühl & Litt 2003). The upper boundary of PAAZ VIb, defined by the increase of NAP to >25% (Müller 1974; Table 1), marks the end of the palynologically defined Eemian. When applying the percentage calculation of Müller (1974), NAP percentages are (almost) continuously >25% only above 2046 cm (Fig. S1). The strong increase of *Sphagnum* and *Calluna* at the end of PAAZ VIb is also clearly visible in the KS 186/70 pollen diagram (Fig. S2). Applying the same average sedimentation rate as in KS 186/70 (~0.74 mm a^{-1}; see section 'Sediment microfacies, varve counting and sedimentation rate estimates'), PAAZ VIb lasted ~1190 years (Table 2).

PAAZ VIc_1+c_2 (high NAP–*Betula–Pinus*; 2046–1819 cm), which biostratigraphically already belongs to the Weichselian, is characterized by the continuing increase of NAP, reaching ~40% at the top of the investigated section (Fig. 5). *Betula* is strongly present (~9–34%) and *Picea* reaches ~1–5%. Cold-tolerant *Salix* and *Juniperus* as well as *Calluna*-dominated heathlands (maximum ~28%) spread while *Pinus* decreases and fluctuates between ~30 and ~50%. Poaceae reach ~5–10% and *Artemisia* and Amaranthaceae occur regularly. High NAP and *Calluna* percentages as well as a strong dominance of *Calluna* over Poaceae are characteristic of the early Weichselian Herning Stadial in northern Germany (Caspers & Freund 2001). Local moisture is indicated by the strong presence of Cyperaceae, fern spores (Fig. S1) and *Sphagnum* (maximum ~23%; the boundary between PAAZ VIc_1 and VIc_2 at 1886 cm is defined by the *Sphagnum* increase to >10%). Low percentages of thermophilous elements (*Carpinus*, *Corylus*, *Alnus*) and sporadic findings of *Ilex* and *Hedera* likely indicate partial reworking of older sediments, which is confirmed by the presence of dinoflagellate cysts and Neogene pollen like *Liquidambar*.

Discussion

Comparison of BIS-2000 and KS 186/70 and implications for the duration of the Eemian in northern Germany

Detailed microfacies analysis revealed that the sub-mm-scale light–dark laminae couplets between 3047 and 2922 cm in BIS-2000 represent carbonaceous-biogenic varves with individual sublayers reflecting season-specific deposition. Sediment microfacies information thereby confirms previous pollen analyses on individual sublayers in the KS 186/70 sediments. These revealed a dominance of pollen from taxa flourishing in early/middle spring (e.g. *Corylus*, *Ulmus*, *Alnus*, *Betula*, *Fraxinus*, *Pinus*, *Quercus*) in the dark sublayers, indicating formation during spring, but most probably including also deposition during the previous autumn and winter (Müller 1974). In contrast, pollen from taxa flourishing in late spring and summer (e.g. *Picea*, *Tilia*, Poaceae, *Artemisia*, *Calluna*) prevailed in the light sublayers, signifying them as predominantly formed during summer (Müller 1974). Given this combined sedimentological and palynological evidence for an annual origin of the sub-mm-scale light–dark laminae couplets, the number of varves/years in the laminated basal part of BIS-2000 and KS 186/70 should be similar. In fact, varve counting and varve counting-based sedimentation rate interpolation yielded a duration of 2098 years for the PAAZ IIa–IIIb section in BIS-2000 (Table 2). This confirms within an uncertainty of <5% the results from KS 186/70, where 2195 years were counted in the same section (Table 2; Müller 1974). Differences in the duration of individual PAAZ between the two sediment cores (Table 2) might be related to the lower resolution of the palynological analyses in BIS-2000 (n = 19) in this interval compared to KS 186/70 (n = 38), affecting the exact positioning of the PAAZ boundaries.

For the faintly/non-varved parts of BIS-2000, i.e. PAAZ I and PAAZ IIIc–VIb, the duration of individual PAAZ was determined by using exactly the same sedimentation rates as those in KS 186/70 (see section 'Sediment microfacies, varve counting and sedimentation rate estimates'). By using this approach, we find – in addition to the close similarity between the two sediment cores for the varve-counted PAAZ IIa–IIIb section – also a good agreement for the thickness/duration of PAAZ 1, which covers 100 years (7 cm) in KS 186/70 and 157 years (11 cm) in BIS-2000, and the PAAZ Va–VIb section, which covers 4000 years (255 cm) in KS 186/70 and ~3800 years (239 cm) in BIS-2000 (in total <4% difference for the duration of these PAAZ between the two sediment cores; Table 2).

In contrast to the good agreement between BIS-2000 and KS 186/70 regarding the thickness/duration of the PAAZ I–IIIb and PAAZ Va–VIb sections documented above (Fig. 7, Table 2), major differences between the two sediment cores are evident in the middle part of the Eemian sediment succession, i.e. in PAAZ IIIc–IVb. While this section covers 303 cm in KS 186/70 (Müller 1974), it includes 578 cm in BIS-2000 (Fig. 7, Table 2). Applying the average sedimentation rates deduced from KS 186/70 to BIS-2000, we find that PAAZ IIIc and IV respectively lasted ~1800 and ~7130 years in BIS-2000 compared to 700 and 4000 years in KS 186/70 (Table 2). As there is no reasonable explanation why the amount of sediment

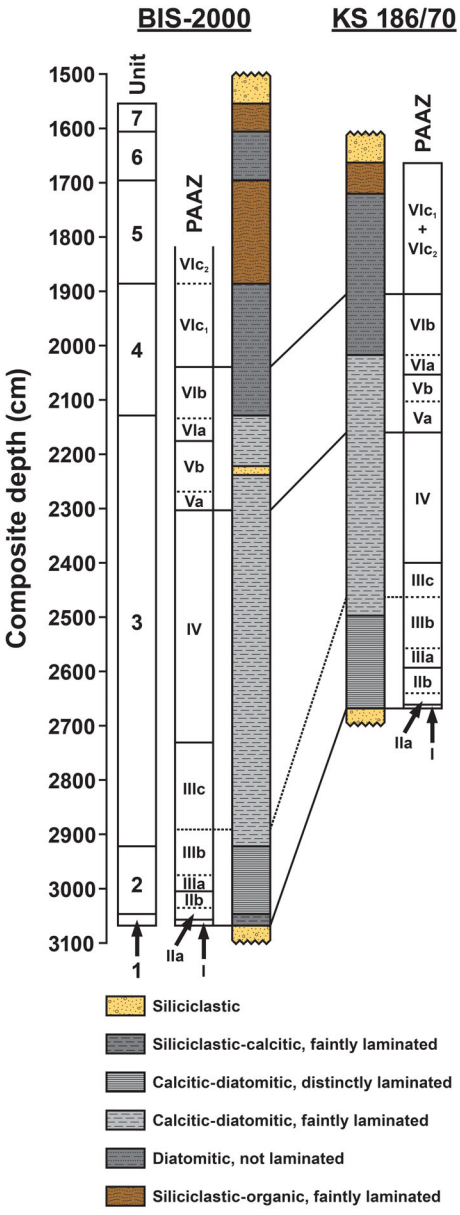

Fig. 7. Comparison of the sedimentology and pollen zonation of sediment cores BIS-2000 and KS 186/70 (Müller 1974) from the Bispingen palaeolake sediment succession. Note that a direct sedimentological comparison between BIS-2000 and KS 186/70 is only possible to a limited extent due to the not very detailed sedimentological description of KS 186/70.

deposited (i.e. the sedimentation rate) at both sites should be fairly identical in the basal and upper part of the sediment succession but significantly different in the middle part, the clearly reduced thickness and consequently also the shorter duration of the PAAZ IIIc–IVb section in KS 186/70 is considered to be very likely related to one or more gaps in the KS 186/70 sediment record in this section. This interpretation is supported by distinct differences between the BIS-2000 and KS 186/70 pollen records. For example, the transition between PAAZ IIIc and IVa in BIS-2000 is characterized by a very gradual increase of *Carpinus* as well as steady declines of *Pinus* and *Corylus*, whereas these changes are very abrupt in KS 186/70. In particular, *Carpinus* increases from <5 to ~35% across ~135 cm in BIS-2000, whereas the same increase in KS 186/70 occurs rather abruptly within only 20 cm (Figs 5, 6). Furthermore, the decrease of *Tilia* in BIS-2000 to <1% occurs rather gradually at the end of PAAZ IVa, whereas this appears to occur earlier in KS 186/70 (Figs 5, 6). These notable differences in individual taxa occurrence between the two sediment cores are very likely indicative of sedimentologically unrecognized gaps in KS 186/70, similar to evidence from other sediment records (e.g. Leroy *et al.* 2000; Kupryjanowicz *et al.* 2023). The occurrence of larger gaps in KS 186/70, which would entail a previous underestimation of the true duration of the Eemian, might be explained by its slightly more marginal location in the former lake basin. The partial loss of larger sections of the KS 186/70 sediment succession could have been caused by local slumping at the steep slopes of the high-relief subglacial channel. This hypothesis is supported by the spatially highly variable thickness of the Bispingen palaeolake sediment succession (Benda & Brandes 1974). Another, and maybe even more reasonable, explanation for gaps in the KS 186/70 sediment succession could be unrecognized loss or non-recovery of sediment during the coring campaign in 1970 as only a single sediment core was obtained back then and not overlapping parallel sediment cores as used for the compilation of BIS-2000.

Taken together, the results of microscopic varve counting for PAAZ IIa–IIIb and the sedimentation rate-based duration estimates for PAAZ I and PAAZ IIIc–VIb determine the length of the entire pollen-defined Eemian in BIS-2000 as ~15 000 years (Table 2) compared to ~11 000 years initially reported for KS 186/70 (see Müller 1974). The new duration estimate of ~15 000 years derived from BIS-2000 must, however, be considered a minimum estimate that could still be biased by the uncertainty of the assumed sedimentation rates in the PAAZ IIIc–VIb section. For example, a reduction of the sedimentation rates in this interval by 15–20% compared to the original estimates derived from KS 186/70 would be sufficient to yield a duration of ~18 000 years for the pollen-defined Eemian at Bispingen, which would be very similar to the duration of the Last Interglacial in southern European records (e.g. Brauer *et al.* 2007; Allen & Huntley 2009; Tzedakis *et al.* 2018).

The revised duration of the Eemian in northern Germany in comparison with other European Last Interglacial proxy records

To date, the most robust estimate for the duration of the pollen-defined Last Interglacial in Europe originates from the varved lake sediment record of Lago Grande di Monticchio, southern Italy. Here, the Last Interglacial lasted 17 700±200 years between 127.2±1.6 and 109.5±1.4 ka BP (Brauer *et al.* 2007; Allen & Huntley 2009; Fig. 8) with a later chronological revision shifting the Last Interglacial by a few hundred years towards older ages, e.g. its end to 110.4±0.7 ka BP (Martin-Puertas *et al.* 2014, 2019). Keeping in mind that vegetation changes at the onset of the Last Interglacial were not necessarily synchronous with climatic shifts observed in $\delta^{18}O$ records, not only the duration but also the absolute dating of the Last Interglacial inferred from the Lago Grande di Monticchio pollen record are confirmed within the dating uncertainty by the recently revised U/Th-dated speleothem $\delta^{18}O$ record from Corchia Cave, northern Italy, where full interglacial climate conditions lasted between 129.0±0.5 and 111.0±0.9 ka BP, i.e. for ~18 000 years (Tzedakis *et al.* 2018; Fig. 8). This age/duration estimate was also transferred to marine sediment core MD01-2444 from the Iberian margin offshore Portugal (Tzedakis *et al.* 2018; Fig. 8), where the duration of the Last Interglacial was previously determined to be ~16 400 years from combined pollen and $\delta^{18}O$ analyses on marine sediment core MD95-2042, placing the start of reforestation at the onset of the Last Interglacial at 126.1 ka BP and the end of the interglacial vegetation succession at 109.7 ka BP (Sánchez Goñi *et al.* 1999; Shackleton *et al.* 2002, 2003). Given the revised chronology for the Iberian margin proxy records and the evidence from Lago Grande di Monticchio and Corchia Cave, Last Interglacial palaeoclimatic/-environmental changes in southern Europe occurred therefore apparently contemporaneously.

The spread of temperate vegetation in Europe at the onset of the Last Interglacial is – despite regional differences in vegetation composition – commonly assumed to have been quasi-synchronous across a wide latitudinal/longitudinal range (Tzedakis 2003), similar to that at the onset of the Holocene (e.g. Brauer *et al.* 1999; Lohne *et al.* 2013; Engels *et al.* 2022). Consequently, the apparent ~2500–3000-year difference between our new minimum duration estimate of ~15 000 years for the Eemian at Bispingen and the latest duration estimates of ~18 000 years from southern Europe (Brauer *et al.* 2007; Allen & Huntley 2009; Tzedakis *et al.* 2018) could reflect a regionally different vegetation development at the demise of the Last

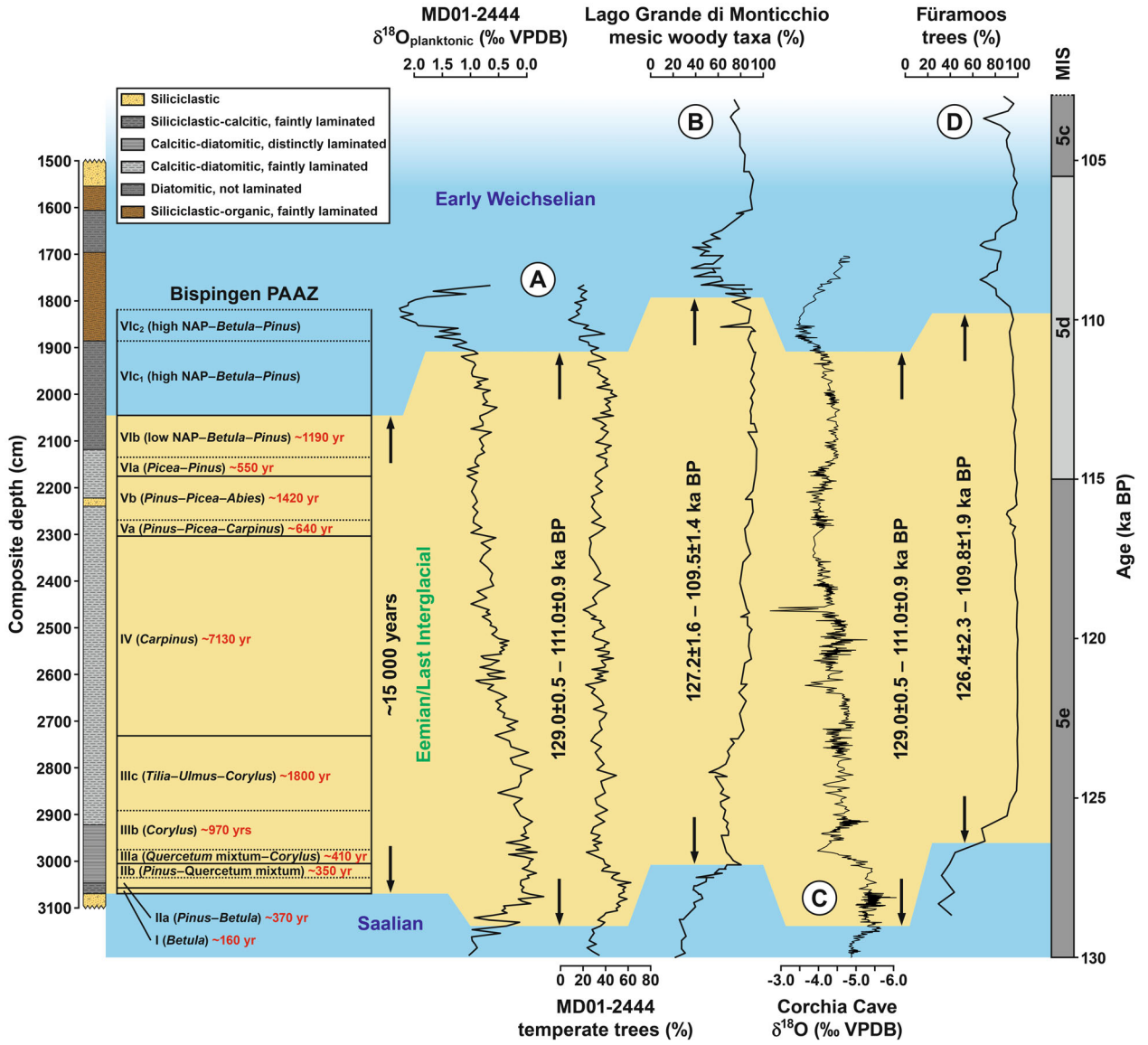

Fig. 8. Comparison of the BIS-2000 pollen zonation (plotted on depth scale) with different European Last Interglacial palaeoclimate proxy records (plotted on their individual time scales; for the location of the individual records see Fig. 1). A. Planktonic foraminifera $\delta^{18}O$ and pollen data from marine sediment core MD01-2444, Iberian margin (Tzedakis *et al.* 2018). B. Pollen data from Lago Grande di Monticchio, southern Italy (Brauer *et al.* 2007; Allen & Huntley 2009). Note that the recent revision of the chronology, which shifted the Last Interglacial towards older ages, now placing its end at 110.4±0.7 ka BP (Martin-Puertas *et al.* 2014, 2019), is not considered here. C. Speleothem $\delta^{18}O$ data from Corchia Cave, northern Italy (Tzedakis *et al.* 2018). D. Pollen data from Füramoos, southern Germany (Kern *et al.* 2022). Note that the chronology of this record is based on tuning to the age model of marine sediment core MD95-2042 from the Iberian margin (Sánchez Goñi *et al.* 1999; Shackleton *et al.* 2002, 2003), while a new chronological framework for sediment records from the Iberian margin was recently proposed by Tzedakis *et al.* (2018).

Interglacial. The existence of such a vegetation gradient between southern and northern-central Europe at the end of the Last Interglacial could be related to the relative proximity of Bispingen to the successively growing Scandinavian ice sheet (see Ehlers & Gibbard 2004). This probably exerted a stronger impact on the vegetation in northern Germany during the final stage of the Last Interglacial, e.g. through stronger winter cooling and reduced precipitation (Kühl *et al.* 2007), terminating the phase of temperate vegetation earlier than at locations further south. However, based on our new floating duration estimate, this phase of contrasting climate conditions between southern and northern-central Europe was significantly shorter than the multi-millennia-long trans-European vegetation gradient that was previously suggested from the comparison between pollen records from France and the initial Last Interglacial duration estimate of ~11 000 years from

Bispingen (Kukla *et al.* 2002b; Tzedakis 2003). Nevertheless, we actually cannot exclude a similar length of the Last Interglacial and therefore synchronous vegetation changes throughout Europe given the uncertainty of the sedimentation rate estimates in the PAAZ IIIc–VIb section of BIS-2000 (see above). Either way, the relatively long dominance of temperate deciduous tree vegetation, particularly *Carpinus*, until ~11 000 years after the onset of the Eemian (i.e. until the end of PAAZ IV) appears notable with respect to the continuous decline in summer insolation since the middle Eemian, which should have been accompanied by decreasing growing season warmth and thus an earlier disappearance of temperate vegetation in northern Europe compared to locations further south (Tzedakis 2003). However, the persistence of *Carpinus* into the terminal phase of the Eemian is also observed at other sites in northern-central Europe (e.g. Erd 1973; Hahne *et al.* 1994; Litt 1994; Pidek *et al.* 2021) as well as at high-altitude sites further south (de Beaulieu & Reille 1992), indicating that in addition to summer insolation/growing season temperature also other factors might have influenced the regional vegetation.

A robust absolute age determination for the Bispingen palaeolake sediment succession is, however, still lacking because absolute dating methods for (palaeo)lake sediments from the Last Interglacial still lack the necessary precision. Although a quasi-synchronous onset (within the dating uncertainty of the individual proxy records) of the pollen-defined Last Interglacial at ~127–129 ka BP is indicated by proxy records from southern Europe (e.g. Brauer *et al.* 2007; Allen & Huntley 2009; Tzedakis *et al.* 2018) (Fig. 8), caution should be exercised in directly transferring this date to the Bispingen pollen record as Last Interglacial vegetation successions from different latitudes and elevations are not necessarily directly comparable (see Sirocko *et al.* 2005). Furthermore, a simple alignment of the Bispingen pollen record with marine sediment and speleothem $\delta^{18}O$ records is also not recommendable as the onset of the Last Interglacial/MIS 5e in marine sediment and speleothem $\delta^{18}O$ records consistently predates the spread of temperate vegetation by up to several millennia (e.g. Shackleton *et al.* 2003; Luetscher *et al.* 2021; Honiat *et al.* 2022). Hence, a robust synchronization of the Bispingen pollen record with other Last Interglacial palaeoclimate archives from Europe remains subject to the identification of isochronous time markers like, for example, cryptotephras.

Conclusions

A continuous record of lacustrine deposition from the onset of the Last Interglacial (Eemian) into the early Last Glacial (Weichselian) is preserved in the partly varved palaeolake sediment succession of Bispingen, northern Germany, representing a unique archive of environmental changes in Europe during one of the warmest interglacials of the last ~800 000 years. Sedimentological and palynological features of the new composite sediment core BIS-2000 from this classic Last Interglacial site are largely consistent with data from the previously investigated sediment core KS 186/70 (Müller 1974). In particular, varve counting and sedimentation rate-based duration estimates reveal a very good agreement for the thickness and duration of individual pollen zones in the lower and upper parts of the two sediment cores. However, the distinctly longer middle part of the Eemian sediment succession (PAAZ IIIc–IVb) in BIS-2000 suggests previously unrecognized gaps of in total ~4000 years duration in KS 186/70. Consequently, the minimum duration of the pollen-defined Last Interglacial in northern Germany is revised to ~15 000 years, which is still ~1500–3000 years shorter than in southern Europe, but substantially longer than previously reported. This goes a long way in resolving previous suggestions of a major asynchrony in vegetation changes across Europe at the demise of the Last Interglacial that were based on the previous estimate of an ~11 000-year-long Eemian at Bispingen.

Acknowledgements. – We thank the GFZ for funding the coring campaign, the Erkelenzer Bohrgesellschaft mbH, Koblenz, Germany, for conducting the coring and Wolfgang Drewes for providing permission to access his property at Bispingen. The Lower Saxony State Office for Geographic Information and Land Development is acknowledged for providing topographic maps. Furthermore, we thank Dieter Berger, Gabriele Arnold (both GFZ) and Michael Köhler (formerly GFZ, now MKfactory) for preparing high-quality sediment thin sections, the late Georg Schettler (GFZ) for carrying out the bulk sediment geochemical analyses, Thomas Litt for facilitating pollen sample preparation at the University of Bonn and Prosper Bande for preparing palynological slides at the University of the Witwatersrand. Jan A. Piotrowski is acknowledged for editorial handling and Chronis Tzedakis and an anonymous reviewer provided constructive comments on earlier versions of the manuscript. Open Access funding enabled and organized by Projekt DEAL.

Author contributions. – SL and AB conceived the study. SL carried out the sediment microfacies analysis and varve counting. RT conducted the XRF core scanning and was responsible for XRF data interpretation. FHN carried out the pollen analyses and related data interpretation and provided first drafts of the section 'Pollen zonation and duration of individual PAAZ' and the pollen diagrams. SL carried out the data synthesis and led the final figure drafting as well as the writing of the manuscript, incorporating contributions from AB, RT and FHN, as well as input from the managing editor and the reviewers.

Data availability statement. – All proxy data from the BIS-2000 composite sediment core presented in this study will be made available via the World Data Center PANGAEA (www.pangaea.de) after final publication.

References

Allen, J. R. M. & Huntley, B. 2009: Last interglacial palaeovegetation, palaeoenvironments and chronology: a new record from Lago Grande di Monticchio, southern Italy. *Quaternary Science Reviews 28*, 1521–1538.

de Beaulieu, J. L. & Reille, M. 1992: Long Pleistocene pollen sequences from the Velay Plateau (Massif Central, France). *Vegetation History and Archaeobotany 1*, 233–242.

Benda, L. & Brandes, H. 1974: Die Kieselgur-Lagerstätten Niedersachsens: I. Verbreitung, Alter und Genese. *Geologisches Jahrbuch A21*, 3–85.

Berglund, B. E. & Ralska-Jasiewiczowa, M. 1986: Pollen analysis and pollen diagrams. *In* Berglund, B. E. (ed.): *Handbook of Holocene Palaeoecology and Palaeohydrology*, 455–484. John Wiley & Sons, Chichester.

Beug, H.-J. 2004: *Leitfaden der Pollenbestimmung für Mitteleuropa und angrenzende Gebiete*. 542 pp. Verlag Dr. Friedrich Pfeil, München.

Bintanja, R., van de Wal, R. S. W. & Oerlemans, J. 2005: Modelled atmospheric temperatures and global sea levels over the past million years. *Nature 437*, 125–128.

Bluszcz, P., Kirilova, E., Lotter, A. F., Ohlendorf, C. & Zolitschka, B. 2008: Global radiation and onset of stratification as forcing factors of seasonal carbonate and organic matter flux dynamics in a hypertrophic hardwater lake (Sacrower See, northeastern Germany). *Aquatic Geochemistry 14*, 73–98.

Bober, A., Pidek, I. A. & Żarski, M. 2018: Late Saalian and Eemian interglacial at the Struga site (Garwolin Plain, central Poland). *Acta Palaeobotanica 58*, 219–229.

Brauer, A. 2004: Annually laminated lake sediments and their palaeoclimatic relevance. *In* Fischer, H., Flöser, G., Kumke, T., Lohmann, G., Miller, H., Negendank, J. F. W. & von Storch, H. (eds.): *The KIHZ Project: Towards a Synthesis of Holocene Proxy Data and Climate Models*, 109–128. Springer Verlag, Berlin.

Brauer, A., Allen, J. R. M., Mingram, J., Dulski, P., Wulf, S. & Huntley, B. 2007: Evidence for last interglacial chronology and environmental change from southern Europe. *Proceedings of the National Academy of Sciences of the United States of America 104*, 450–455.

Brauer, A., Endres, C., Günter, C., Litt, T., Stebich, M. & Negendank, J. F. W. 1999: High resolution sediment and vegetation responses to Younger Dryas climate change in varved lake sediments from Meerfelder Maar, Germany. *Quaternary Science Reviews 18*, 321–329.

Brauer, A., Mangili, C., Moscariello, A. & Witt, A. 2008: Palaeoclimatic implications from micro-facies data of a 5900 varve time series from the Pànico interglacial sediment record, southern Alps. *Palaeogeography, Palaeoclimatology, Palaeoecology 259*, 121–135.

Brunskill, G. J. 1969: Fayetteville Green Lake, New York. II. Precipitation and sedimentation of calcite in a meromictic lake with laminated sediments. *Limnology and Oceanography 14*, 830–847.

Caspers, G. & Freund, H. 2001: Vegetation and climate in the early- and pleni-Weichselian in northern Central Europe. *Journal of Quaternary Science 16*, 31–48.

Drysdale, R. N., Zanchetta, G., Hellstrom, J. C., Fallick, A. E., McDonald, J. & Cartwright, I. 2007: Stalagmite evidence for the precise timing of North Atlantic cold events during the early last glacial. *Geology 35*, 77–80.

Drysdale, R. N., Zanchetta, G., Hellstrom, J. C., Fallick, A. E. & Zhao, J.-X. 2005: Stalagmite evidence for the onset of the Last Interglacial in southern Europe at 129 ± 1 ka. *Geophysical Research Letters 32*, L24708, https://doi.org/10.1029/2005GL024658.

Dutton, A. & Lambeck, K. 2012: Ice volume and sea level during the Last Interglacial. *Science 337*, 216–219.

Ehlers, J. & Gibbard, P. L. 2004: *Quaternary Glaciations: Extent and Chronology, Part 1: Europe*. 488 pp. Elsevier, Amsterdam.

Ehlers, J., Eissmann, L., Lippstreu, L., Stephan, H.-J. & Wansa, S. 2004: Pleistocene glaciations of North Germany. *In* Ehlers, J. & Gibbard, P. L. (eds.): *Quaternary Glaciations: Extent and Chronology, Part 1: Europe*, 135–146. Elsevier, Amsterdam.

Engels, S., Lane, C. S., Haliuc, A., Hoek, W. Z., Muschitiello, F., Baneschi, I., Bouwman, A., Bronk Ramsey, C., Collins, J., de Bruijn, R., Heiri, O., Hubay, K., Jones, G., Laug, A., Merkt, J., Müller, M., Peters, T., Peterse, F., Staff, R. A., ter Schure, A. T. M., Turner, F., van den Bos, V. & Wagner-Cremer, F. 2022: Synchronous vegetation response to the last glacial-interglacial transition in northwest Europe. *Communications Earth & Environment 3*, 130, https://doi.org/10.1038/s43247-022-00457-y.

Erd, K. 1973: Pollenanalytische Gliederung des Pleistozäns der Deutschen Demokratischen Republik. *Zeitschrift für Geologische Wissenschaften 1*, 1087–1103.

Fischer, H., Meissner, K. J., Mix, A. C., Abram, N. J., Austermann, J., Brovkin, V., Capron, E., Colombaroli, D., Daniau, A.-L., Dyez, K. A., Felis, T., Finkelstein, S. A., Jaccard, S. L., McClymont, E. L., Rovere, A., Sutter, J., Wolff, E. W., Affolter, S., Bakker, P., . . . Zhou, L. 2018: Palaeoclimate constraints on the impact of 2 °C anthropogenic warming and beyond. *Nature Geoscience 11*, 474–485.

Fox-Kemper, B., Hewitt, H. T., Xiao, C., Aðalgeirsdóttir, G., Drijfhout, S. S., Edwards, T. L., Golledge, N. R., Hemer, M., Kopp, R. E., Krinner, G., Mix, A., Notz, D., Nowicki, S., Nurhati, I. S., Ruiz, L., Sallée, J.-B., Slangen, A. B. A. & Yu, Y. 2021: Ocean, Cryosphere and Sea level change. *In* Masson-Delmotte, V., Zhai, P., Pirani, A., Connors, S. L., Péan, C., Berger, S., Caud, N., Chen, Y., Goldfarb, L., Gomis, M. I., Huang, M., Leitzell, K., Lonnoy, E., Matthews, J. B. R., Maycock, T. K., Waterfield, T., Yelekçi, O., Yu, R. & Zhou, B. (eds.): *Climate Change 2021: The Physical Science Basis. Contribution of Working Group I to the Sixth Assessment Report of the Intergovernmental Panel on Climate Change*, 1211–1362. Cambridge University Press, Cambridge and New York.

Geyh, M. A., Merkt, J. & Müller, H. 1971: Sediment-, Pollen-, und Isotopenanalysen an jahreszeitlich geschichteten Ablagerungen im zentralen Teil des Schleinsees. *Archiv für Hydrobiologie 69*, 366–399.

Grimm, E. C. 1992: TILIA and TILIA GRAPH: pollen spreadsheet and graphics programs. 8th International Palynological Congress. Aix-en-Provence, Program and Abstracts, p. 56.

Hahne, J., Kemle, S., Merkt, J. & Meyer, K.-D. 1994: Eem-, weichsel- und saalezeitliche Ablagerungen der Bohrung "Quakenbrück GE 2". *Geologisches Jahrbuch A134*, 9–69.

Honiat, C., Festi, D., Wilcox, P. S., Edwards, R. L., Cheng, H. & Spötl, C. 2022: Early Last Interglacial environmental changes recorded by speleothems from Katerloch (south-east Austria). *Journal of Quaternary Science 37*, 664–676.

Iversen, J. 1944: *Viscum*, *Hedera* and *Ilex* as climate indicators. *Geologiska Föreningen i Stockholm Förhandlingar 66*, 463–483.

Kelts, K. & Hsü, K. J. 1978: Freshwater carbonate sedimentation. *In* Lerman, A. (ed.): *Lakes: Chemistry, Geology, Physics*, 295–324. Springer, New York.

Kern, O. A., Koutsodendris, A., Allstädt, F. J., Mächtle, B., Peteet, D. M., Kalaitzidis, S., Christanis, K. & Pross, J. 2022: A near-continuous record of climate and ecosystem variability in Central Europe during the past 130 kyrs (Marine Isotope Stages 5–1) from Füramoos, southern Germany. *Quaternary Science Reviews 284*, 107505, https://doi.org/10.1016/j.quascirev.2022.107505.

Kołaczek, P., Karpińska-Kołaczek, M. & Petera-Zganiacz, J. 2012: Vegetation patterns under climate changes in the Eemian and Early Weichselian in Central Europe inferred from a palynological sequence from Ustków (central Poland). *Quaternary International 268*, 9–20.

Kühl, N. & Litt, T. 2003: Quantitative time series reconstruction of Eemian temperature at three European sites using pollen data. *Vegetation History and Archaeobotany 12*, 205–214.

Kühl, N., Litt, T., Schölzel, C. & Hense, A. 2007: Eemian and Early Weichselian temperature and precipitation variability in northern Germany. *Quaternary Science Reviews 26*, 3311–3317.

Kukla, G. J., de Beaulieu, J.-L., Svobodova, H., Andrieu-Ponel, V., Thouveny, N. & Stockhausen, H. 2002a: Tentative correlation of pollen records of the last interglacial at Grande Pile and Ribains with marine isotope stages. *Quaternary Research 58*, 32–35.

Kukla, G. J., Bender, M. L., de Beaulieu, J.-L., Bond, G. C., Broecker, W. S., Cleveringa, P., Gavin, J. E., Herbert, T. D., Imbrie, J., Jouzel, J., Keigwin, L. D., Knudsen, K. L., McManus, J. F., Merkt, J., Muhs, D. R., Müller, H., Poore, R. Z., Porter, S. C., Seret, G., Shackleton, N. J., Turner, C., Tzedakis, P. C. & Winograd, I. J. 2002b: Last interglacial climates. *Quaternary Research 58*, 2–13.

Kukla, G., McManus, J. F., Rousseau, D.-D. & Chuine, I. 1997: How long and how stable was the last interglacial? *Quaternary Science Reviews 16*, 605–612.

Kupryjanowicz, M., Fiłoc, M., Woronko, B., Karasiewicz, T. M., Rychel, J., Adamczyk, A. & Jarosz, J. 2021: Eemian and early Weichselian environmental changes at the Jałówka site, NE Poland,

and their correlation with marine and ice records. *Quaternary Research 104*, 69–88.
Kupryjanowicz, M., Fiłoc, M., Żuk-Kempa, E. & Żarski, M. 2023: Are several profiles better than one? Multi-profile palynological study of the Eemian lacustrine sediments at the Wola Starogrodzka site (Garwolin Plain, Central Poland). *Acta Geologica Polonica 73*, 411–431.
Lauterbach, S., Brauer, A., Andersen, N., Danielopol, D. L., Dulski, P., Hüls, M., Milecka, K., Namiotko, T., Obremska, M., von Grafenstein, U. & DecLakes Participants 2011: Environmental responses to Lateglacial climatic fluctuations recorded in the sediments of pre-Alpine Lake Mondsee (northeastern Alps). *Journal of Quaternary Science 26*, 253–267.
Lauterbach, S., Mingram, J., Schettler, G. & Orunbaev, S. 2019: Two twentieth-century M_{LH} = 7.5 earthquakes recorded in annually laminated lake sediments from Sary Chelek, western Tian Shan, Kyrgyzstan. *Quaternary Research 92*, 288–303.
Leroy, S. A. G., Zolitschka, B., Negendank, J. F. W. & Seret, G. 2000: Palynological analyses in the laminated sediment of Lake Holzmaar (Eifel, Germany): duration of Lateglacial and Preboreal biozones. *Boreas 29*, 52–71.
Litt, T. 1994: Paläoökologie, Paläobotanik und Stratigraphie des Jungquartärs im nordmitteleuropäischen Tiefland unter besonderer Berücksichtigung des Elbe-Saale-Gebietes. *Dissertationes Botanicae 227*, 1–185.
Lohne, Ø. S., Mangerud, J. & Birks, H. H. 2013: Precise ^{14}C ages of the Vedde and Saksunarvatn ashes and the Younger Dryas boundaries from western Norway and their comparison with the Greenland Ice Core (GICC05) chronology. *Journal of Quaternary Science 28*, 490–500.
Lotter, A. F. 1989: Evidence of annual layering in Holocene sediments of Soppensee, Switzerland. *Aquatic Sciences 51*, 19–31.
Luetscher, M., Moseley, G. E., Festi, D., Hof, F., Edwards, R. L. & Spötl, C. 2021: A Last Interglacial speleothem record from the Sieben Hengste cave system (Switzerland): implications for alpine paleovegetation. *Quaternary Science Reviews 262*, 106974, https://doi.org/10.1016/j.quascirev.2021.106974.
Maier, D. B., Gälman, V., Renberg, I. & Bigler, C. 2018: Using a decadal diatom sediment trap record to unravel seasonal processes important for the formation of the sedimentary diatom signal. *Journal of Paleolimnology 60*, 133–152.
Malkiewicz, M. 2018a: A Late Saalian Glaciation, Eemian Interglacial and Early Weichselian pollen sequence at Szklarka, SW Poland – reconstruction of vegetation and climate. *Quaternary International 467*, 43–53.
Malkiewicz, M. 2018b: Pollen-based vegetation and climate reconstruction of the Eemian sequence from Buntowo, N Poland. *Quaternary International 467*, 54–61.
Mamakowa, K. 1989: Late middle Polish glaciation, Eemian and early Vistulian vegetation at Imbramowice near Wrocław and the pollen stratigraphy of this part of the Pleistocene in Poland. *Acta Palaeobotanica 29*, 11–176.
Martin-Puertas, C., Brauer, A., Wulf, S., Ott, F., Lauterbach, S. & Dulski, P. 2014: Annual proxy data from Lago Grande di Monticchio (southern Italy) between 76 and 112 ka: new chronological constraints and insights on abrupt climatic oscillations. *Climate of the Past 10*, 2099–2114.
Martin-Puertas, C., Lauterbach, S., Allen, J. R. M., Perez, M., Blockley, S., Wulf, S., Huntley, B. & Brauer, A. 2019: Initial Mediterranean response to major climate reorganization during the last interglacial-glacial transition. *Quaternary Science Reviews 215*, 232–241.
Menke, B. & Tynni, R. 1984: Das Eeminterglazial und das Weichselfrühglazial von Rederstall/Dithmarschen und ihre Bedeutung für die mitteleuropäische Jungpleistozän-Gliederung. *Geologisches Jahrbuch A76*, 1–120.
Meyers, P. A. & Lallier-Vergès, E. 1999: Lacustrine sedimentary organic matter records of late Quaternary paleoclimates. *Journal of Paleolimnology 21*, 345–372.
Milner, A. M., Müller, U. C., Roucoux, K. H., Collier, R. E. L., Pross, J., Kalaitzidis, S., Christanis, K. & Tzedakis, P. C. 2013: Environmental variability during the Last Interglacial: a new high-resolution pollen record from Tenaghi Philippon, Greece. *Journal of Quaternary Science 28*, 113–117.
Müller, H. 1974: Pollenanalytische Untersuchungen und Jahresschichtenzählung an der eem-zeitlichen Kieselgur von Bispingen/Luhe. *Geologisches Jahrbuch A21*, 149–169.
Past Interglacials Working Group of PAGES 2016: Interglacials of the last 800,000 years. *Reviews of Geophysics 54*, 162–219.
Pidek, I. A., Zalat, A. A., Hrynowiecka, A. & Żarski, M. 2021: A high-resolution pollen and diatom record of mid-to late-Eemian at Kozłów (Central Poland) reveals no drastic climate changes in the hornbeam phase of this interglacial. *Quaternary International 583*, 14–30.
Punt, W. 1976: *The Northwest European Pollen Flora, Volume I*. 152 pp. Elsevier, Amsterdam.
Punt, W. & Blackmore, S. 1991: *The Northwest European Pollen Flora, Volume VI*. 275 pp. Elsevier, Amsterdam.
Punt, W. & Clarke, G. C. S. 1980: *The Northwest European Pollen Flora, Volume II*. 274 pp. Elsevier, Amsterdam.
Punt, W. & Clarke, G. C. S. 1981: *The Northwest European Pollen Flora, Volume III*. 144 pp. Elsevier, Amsterdam.
Punt, W. & Clarke, G. C. S. 1984: *The Northwest European Pollen Flora, Volume IV*. 376 pp. Elsevier, Amsterdam.
Punt, W., Blackmore, S. & Clarke, G. C. S. 1988: *The Northwest European Pollen Flora, Volume V*. 154 pp. Elsevier, Amsterdam.
Punt, W., Blackmore, S. & Hoen, P. P. 1995: *The Northwest European Pollen Flora, Volume VII*. 282 pp. Elsevier, Amsterdam.
Punt, W., Blackmore, S., Hoen, P. P. & Stafford, P. J. 2003: *The Northwest European Pollen Flora, Volume VIII*. 192 pp. Elsevier, Amsterdam.
Roeser, P., Dräger, N., Brykała, D., Ott, F., Pinkerneil, S., Gierszewski, P., Lindemann, C., Plessen, B., Brademann, B., Kaszubski, M., Fojutowski, M., Schwab, M. J., Słowiński, M., Błaszkiewicz, M. & Brauer, A. 2021: Advances in understanding calcite varve formation: new insights from a dual lake monitoring approach in the southern Baltic lowlands. *Boreas 50*, 419–440.
Salonen, J. S., Helmens, K. F., Brendryen, J., Kuosmanen, N., Väliranta, M., Goring, S., Korpela, M., Kylander, M., Philip, A., Plikk, A., Renssen, H. & Luoto, M. 2018: Abrupt high-latitude climate events and decoupled seasonal trends during the Eemian. *Nature Communications 9*, 2851, https://doi.org/10.1038/s41467-018-05314-1.
Sánchez Goñi, M. F., Eynaud, F., Turon, J. L. & Shackleton, N. J. 1999: High resolution palynological record off the Iberian margin: direct land-sea correlation for the last interglacial complex. *Earth and Planetary Science Letters 171*, 123–137.
Sánchez Goñi, M. F., Landais, A., Fletcher, W. J., Naughton, F., Desprat, S. & Duprat, J. 2008: Contrasting impacts of Dansgaard-Oeschger events over a western European latitudinal transect modulated by orbital parameters. *Quaternary Science Reviews 27*, 1136–1151.
Schneider, R., Schmitt, J., Köhler, P., Joos, F. & Fischer, H. 2013: A reconstruction of atmospheric carbon dioxide and its stable carbon isotopic composition from the penultimate glacial maximum to the last glacial inception. *Climate of the Past 9*, 2507–2523.
Selle, W. 1962: Geologische und vegetationskundliche Untersuchungen an einigen wichtigen Vorkommen des letzten Interglazials in Nordwestdeutschland. *Geologisches Jahrbuch 79*, 295–352.
Shackleton, N. J. 1969: The Last Interglacial in the marine and terrestrial records. *Proceedings of the Royal Society of London. Series B. Biological Sciences 174*, 135–154.
Shackleton, N. J., Chapman, M., Sánchez Goñi, M. F., Pailler, D. & Lancelot, Y. 2002: The classic marine isotope substage 5e. *Quaternary Research 58*, 14–16.
Shackleton, N. J., Sánchez Goñi, M. F., Pailler, D. & Lancelot, Y. 2003: Marine isotope substage 5e and the Eemian Interglacial. *Global and Planetary Change 36*, 151–155.
Sinopoli, G., Masi, A., Regattieri, E., Wagner, B., Francke, A., Peyron, O. & Sadori, L. 2018: Palynology of the Last Interglacial Complex at Lake Ohrid: palaeoenvironmental and palaeoclimatic inferences. *Quaternary Science Reviews 180*, 177–192.
Sirocko, F., Seelos, K., Schaber, K., Rein, B., Dreher, F., Diehl, M., Lehne, R., Jaeger, K., Krbetschek, M. & Degering, D. 2005: A late

Eemian aridity pulse in Central Europe during the last glacial inception. *Nature 436*, 833–836.
Suchora, M., Kultys, K., Stachowicz-Rybka, R., Pidek, I. A., Hrynowiecka, A., Terpiłowski, S., Łabęcka, K. & Żarski, M. 2022: Palaeoecological record of long Eemian series from Kozłów (Central Poland) with reference to palaeoclimatic and palaeohydrological interpretation. *Quaternary International 632*, 36–50.
Tjallingii, R., Röhl, U., Kölling, M. & Bickert, T. 2007: Influence of the water content on X-ray fluorescence core-scanning measurements in soft marine sediments. *Geochemistry, Geophysics, Geosystems 8*, Q02004, https://doi.org/10.1029/2006GC001393.
Turner, C. 2002: Problems of the duration of the Eemian interglacial in Europe north of the Alps. *Quaternary Research 58*, 45–48.
Tylmann, W., Enters, D., Kinder, M., Moska, P., Ohlendorf, C., Poręba, G. & Zolitschka, B. 2013: Multiple dating of varved sediments from Lake Łazduny, northern Poland: toward an improved chronology for the last 150 years. *Quaternary Geochronology 15*, 98–107.
Tzedakis, C. 2003: Timing and duration of last interglacial conditions in Europe: a chronicle of a changing chronology. *Quaternary Science Reviews 22*, 763–768.
Tzedakis, P. C., Drysdale, R. N., Margari, V., Skinner, L. C., Menviel, L., Rhodes, R. H., Taschetto, A. S., Hodell, D. A., Crowhurst, S. J., Hellstrom, J. C., Fallick, A. E., Grimalt, J. O., McManus, J. F., Martrat, B., Mokeddem, Z., Parrenin, F., Regattieri, E., Roe, K. & Zanchetta, G. 2018: Enhanced climate instability in the North Atlantic and southern Europe during the Last Interglacial. *Nature Communications 9*, 4235, https://doi.org/10.1038/s41467-018-06683-3.
Tzedakis, P. C., Frogley, M. R. & Heaton, T. H. E. 2003: Last interglacial conditions in southern Europe: evidence from Ioannina, northwest Greece. *Global and Planetary Change 36*, 157–170.
Weltje, G. J. & Tjallingii, R. 2008: Calibration of XRF core scanners for quantitative geochemical logging of sediment cores: theory and application. *Earth and Planetary Science Letters 274*, 423–438.
Wilcox, P. S., Honiat, C., Trüssel, M., Edwards, R. L. & Spötl, C. 2020: Exceptional warmth and climate instability occurred in the European Alps during the Last Interglacial period. *Nature Communications Earth & Environment 1*, 57, https://doi.org/10.1038/s43247-020-00063-w.
Zagwijn, W. H. 1996: An analysis of Eemian climate in Western and Central Europe. *Quaternary Science Reviews 15*, 451–469.
Zolitschka, B., Francus, P., Ojala, A. E. K. & Schimmelmann, A. 2015: Varves in lake sediments – a review. *Quaternary Science Reviews 117*, 1–41.

Supporting Information

Additional Supporting Information to this article is available at http://www.boreas.dk.

Fig. S1. Simplified pollen diagram of BIS-2000 using the percentage calculation of Müller (1974). The boundaries of individual PAAZ follow the criteria used for KS 186/70 (Müller 1974; Table 1).

Fig. S2. Simplified pollen diagram of KS 186/70 using the percentage calculation of Müller (1974). The pollen count data are available at the European Pollen Database (https://epdweblog.org) via the Neotoma Paleoecology Database (http://www.neotomadb.org; dataset ID 40169).